A membrane-depolarizing toxin substrate of the *Staphylococcus aureus* Type VII secretion system mediates intra-species competition

Fatima R. Ulhuq[a], Margarida C. Gomes[b,c], Gina Duggan[b,c], Manman Guo[d], Chriselle Mendonca[a,], Grant Buchanan[a], James D. Chalmers[e,f], Zhenping Cao[e], Holger Kneuper[e], Sarah Murdoch[e], Sarah Thomson[g], Henrik Strahl[a], Matthias Trost[d,h], Serge Mostowy[b,c,1] and Tracy Palmer[a,1]

[a]Molecular and Cellular Microbiology Theme, Newcastle University Biosciences Institute, Newcastle University, Newcastle upon Tyne, NE2 4HH, UK

[b]Section of Microbiology, MRC Centre for Molecular Bacteriology and Infection, Imperial College London, Armstrong Road, London SW7 2AZ, UK

[c]Department of Infection Biology, London School of Hygiene & Tropical Medicine, Keppel Street, London WC1E 7HT, UK

[d]MRC Protein Phosphorylation and Ubiquitylation Unit, School of Life Sciences, University of Dundee, Dundee DD1 5EH, UK

[e]Division of Molecular Microbiology, School of Life Sciences, University of Dundee, Dundee DD1 5EH, UK

[f]Division of Molecular and Clinical Medicine, University of Dundee, Dundee, DD1 9SY, UK

[g]Biological Services, School of Life Sciences, University of Dundee, Dundee DD1 5EH, UK

[h]Newcastle University Biosciences Institute, Newcastle University, Newcastle upon Tyne, NE2 4HH, UK

[1]for correspondence tracy.palmer@newcastle.ac.uk or serge.mostowy@lshtm.ac.uk

Abstract

The type VII protein secretion system (T7SS) is conserved across *Staphylococcus aureus* strains and plays important roles in virulence and interbacterial competition. To date only one T7SS substrate protein, encoded in a subset of *S. aureus* genomes, has been functionally characterized. Here, using an unbiased proteomic approach, we identify TspA as a further T7SS substrate. TspA is encoded distantly from the T7SS gene cluster and is found across all *S. aureus* strains as well as in *Listeria* and Enterococci. Heterologous expression of TspA from *S. aureus* strain RN6390 indicates its C-terminal domain is toxic when targeted to the *Escherichia coli* periplasm and that it depolarizes the cytoplasmic membrane. The membrane depolarizing activity is alleviated by co-production of the membrane-bound TsaI immunity protein, which is encoded adjacent to *tspA* on the *S. aureus* chromosome. Using a zebrafish hindbrain ventricle infection model, we demonstrate that the T7SS of strain RN6390 promotes bacterial replication *in vivo*, and deletion of *tspA* leads to increased bacterial clearance. The toxin domain of TspA is highly polymorphic and *S. aureus* strains encode multiple *tsaI* homologues at the *tspA* locus, suggestive of additional roles in intra-species competition. In agreement, we demonstrate TspA-dependent growth inhibition of RN6390 by strain COL in the zebrafish infection model that is alleviated by the presence of TsaI homologues.

Keywords

Type VII secretion system, *Staphylococcus aureus*, zebrafish, membrane-depolarizing toxin, bacterial competition

Significance statement

Staphylococcus aureus, a human commensal organism that asymptomatically colonizes the nares, is capable of causing serious disease following breach of the mucosal barrier. *S. aureus* strains encode a Type VII secretion system (T7SS) that is required for virulence in mouse infection models, and some strains also secrete a nuclease toxin by this route that has antibacterial activity. Here we identify TspA, widely found in Staphylococci and other

57 pathogenic bacteria, as a T7 substrate. We show that TspA has membrane-depolarizing
58 activity and that *S. aureus* uses TspA to inhibit the growth of a bacterial competitor *in vivo*.
59

60 **Introduction**

61 The Type VII secretion system (T7SS) has been characterized in bacteria of the actinobacteria
62 and firmicutes phyla. In pathogenic mycobacteria the ESX-1 T7SS secretes numerous
63 proteins that are essential for virulence and immune evasion[1]. The Ess T7SS of
64 *Staphylococcus aureus* is also required for pathogenesis in murine models of infection[2-4], and
65 a longitudinal study of persistent *S. aureus* infection in the airways of a cystic fibrosis patient
66 showed that the *ess* T7SS genes were highly upregulated during a 13 year timespan[5]. It is
67 becoming increasingly apparent, however, that in addition to having anti-eukaryotic activity,
68 the T7SS of firmicutes mediates interbacterial competition[6-8]. Some strains of *S. aureus*
69 secrete a DNA endonuclease toxin, EsaD[6, 9], that when overproduced leads to growth
70 inhibition of a sensitive *S. aureus* strain[6]. Moreover, *Streptococcus intermedius* exports at
71 least three LXG domain-containing toxins, TelA, TelB and TelC that mediate contact-
72 dependent growth inhibition against a range of Gram-positive species[7].

73 A large integral membrane ATPase of the FtsK/SpoIIIE family, termed EssC in firmicutes, is a
74 conserved component of all T7SSs and probably energizes protein secretion as well as
75 forming part of the translocation channel[10-15]. EsxA, a small secreted protein of the WXG100
76 family, is a further conserved T7 component that is dependent on the T7SS for its translocation
77 across the membrane[2, 16]. In firmicutes three further membrane proteins, EsaA, EssA and
78 EssB, function alongside the EssC ATPase to mediate T7 protein secretion[17, 18]. In *S. aureus*
79 the T7 structural components are encoded at the *ess* locus. In commonly-studied strains
80 including Newman, RN6390 and USA300, the T7 substrates EsxB, EsxC, EsxD and EsaD are
81 encoded immediately downstream of *essC* (Fig 1A) and are co-regulated with the genes
82 coding for machinery components[2, 3, 6, 9, 19, 20]. With the exception of EsaD the biological
83 activities of these substrates are unknown, although mutational studies have suggested that
84 EsxB and EsxC contribute to persistent infection in a murine abscess model[2, 19].

85 Despite the *ess* locus forming part of the core *S. aureus* genome, these four substrate proteins
86 are not conserved across *S. aureus* isolates, being found in only approximately 50% of
87 sequenced strains[21]. Furthermore, inactivation of the T7SS in *S. aureus* strain ST398 shows

88 a similar decrease in kidney abscess formation as that seen for T7 mutants in Newman and
89 USA300[2, 4, 22], despite the fact that recognizable homologues of EsxB, EsxC, EsxD and EsaD
90 are not encoded by this strain[21]. This strongly suggests that there are further *S. aureus* T7
91 substrates that are yet to be identified. Here we have taken an unbiased approach to identify
92 T7 substrates using quantitative proteomic analysis of culture supernatants from *S. aureus*
93 RN6390 wild type and *essC* strains. We identify a new substrate, TspA that is encoded
94 distantly from the *ess* gene cluster and is found in all sequenced *S. aureus* strains. Further
95 analysis indicates that TspA has a toxic C-terminal domain that depolarizes membranes.
96 Using a zebrafish hindbrain ventricle infection model, we reveal that the T7SS and TspA
97 contribute to both bacterial replication and interbacterial competition *in vivo*.

98 **Results**

99 **The *S. aureus* RN6390 T7SS secreted proteome**

100 To identify candidate T7 substrates, RN6390 and an isogenic *essC* deletion strain[3] were
101 cultured in the minimal medium RPMI. Both strains grew identically (Fig 1B) and expressed
102 components of the T7SS, and as expected secretion of EsxA was abolished in the *essC* strain
103 (Fig 1C). Culture supernatants were isolated when cells reached OD_{600nm} of 1, and label-free
104 quantitative proteomics used to assess changes in protein abundance of four biological
105 replicates of each secretome. Following identification of 1170 proteins, 17 proteins showed,
106 with high confidence ($p < 0.05$, 2-fold change), a decrease in abundance in the secretome of
107 the *essC* strain relative to the RN6390 parent strain (Fig 1D,Table 1; *SI Appendix*, Table S1).

108 Proteomic analysis indicated that the secreted core component, EsxA, was significantly
109 reduced in abundance in the *essC* secretome, as expected from the western blot analysis (Fig
110 1C). Peptides from the membrane-bound T7 component EsaA, which has a large surface-
111 exposed loop[23], were also less abundant in the supernatant of the *essC* strain, as were EsxD
112 and EsaD, known substrates of the T7SS[6, 9, 20] (Table 1, *SI Appendix*, Table S1). The EsxC
113 substrate[19] was also exclusively detected in the supernatant of the wild type strain, but only
114 two EsxC peptides were detected and it did not meet the $p < 0.01$ cut-off (*SI Appendix*, Table
115 S1). EsxB, another previously identified substrate[2, 24], and EsaE, which is co-secreted with
116 EsaD[6] were not detected in any of our analysis.

117 After EsxD, the protein with the highest relative abundance in the secretome of the wild type
118 strain was the uncharacterized protein SAOUHSC_00584. This protein harbors a predicted
119 LXG domain which is common to some T7SS substrates[7]. Other proteins enriched in the
120 secretome of the wild type strain include a predicted superantigen (SAOUHSC_00389), the
121 secretory antigen SsaA, two predicted membrane-bound lipoproteins (SAOUHSC_01180 and
122 SAOUHSC_02695), two uncharacterized proteins (SAOUHSC_00406 and
123 SAOUHSC_02448) and several predicted cytoplasmic proteins (Table 1). A small number of

124 proteins were found to be enriched in abundance in the *essC* secretome (*SI Appendix*, Table
125 S1), including the heme oxygenase IsdI, which is known to be upregulated when the T7SS is
126 inactivated[25].

127

128 **SAOUHSC_00584/TspA localizes to the membrane dependent on EssC**

129 We next constructed tagged variants of each of SAOUHSC_00389, SAOUHSC_00406,
130 SAOUHSC_00584, SAOUHSC_02448 and SsaA to probe their subcellular locations in the
131 wild type and Δ*essC* strains. C-terminally HA-tagged SAOUHSC_00389, SAOUHSC_02448
132 and SsaA were secreted into the culture supernatant in an *essC*-independent manner (*SI*
133 *Appendix*, Fig S1), indicating that these proteins are not substrates of the T7SS and their
134 reduced abundance in the *essC* secretome may arise for pleiotropic reasons. Overproduction
135 of C-terminally Myc-tagged SAOUHSC_00406 caused cell lysis, seen by the presence of TrxA
136 in the supernatant samples (*SI Appendix*, Fig S1B). By contrast, a C-terminally Myc-tagged
137 variant of SAOUHSC_00584 was detected only in the cellular fraction (*SI Appendix*, Fig S1C).
138 To probe the subcellular location of SAOUHSC_00584-Myc, we generated cell wall,
139 membrane and cytoplasmic fractions. Fig 2A shows that the tagged protein localized to the
140 membrane and that it appears to be destabilized by the loss of EssC. SAOUHSC_00584 was
141 subsequently renamed TspA (Type Seven dependent Protein A).

142 TspA is predicted to be 469 amino acids long and to have either one (TMHMM) or two
143 (Predictprotein.org) transmembrane domains towards its C-terminal end. To determine
144 whether it is an integral membrane protein we treated membranes with urea which removes
145 peripherally bound proteins by denaturation. Fig 2B indicates that a large fraction of TspA-Myc
146 was displaced from the membrane to the cytoplasmic fraction by the addition of urea whereas
147 a *bona fide* integral membrane protein, $EssB^{64-28}$, was not displaced by this treatment. We
148 conclude that TspA-Myc peripherally interacts with the membrane. This is consistent with

149 findings from the proteomic experiment as peptides along the entire length of TspA were
150 detected in the secretome (*SI Appendix*, Fig S2).

151 To determine whether TspA-Myc is exposed at the extracellular side we prepared
152 spheroplasts and treated them with proteinase K. Fig 2C shows that at low concentrations of
153 proteinase K, TspA-Myc was proteolytically cleaved to release a smaller fragment that also
154 cross-reacted with the anti-Myc antibody. At least part of this smaller fragment must be
155 extracellular as it was also degraded as the protease concentration was increased. An
156 approximately 37 kDa C-terminal fragment of TspA-Myc detected natively in the absence of
157 added protease was also extracellular as it was sensitive to digestion by proteinase K. The
158 likely topology of TspA is shown in Fig 2E.

159 All *S. aureus* T7SS substrate proteins identified to date are found only in a subset of strains,
160 and are linked with specific *essC* subtypes. However, TspA is encoded by all *S. aureus*
161 genomes examined in Warne *et al.*[21], and is distant from the *ess* locus. This raised the
162 possibility that TspA may be a further secreted core component of the T7 machinery. To
163 examine this, we constructed an in-frame *tspA* deletion in RN6390 and investigated the
164 subcellular location of the T7 secreted component EsxA and the substrate protein EsxC. Fig
165 2D shows that both EsxA and EsxC are secreted in the absence of TspA. We conclude that
166 TspA is a peripheral membrane protein substrate of the T7SS whose localization and/or
167 stability at the extracellular side of the membrane is dependent on EssC, and that it is not a
168 core component of the T7SS.

169

170 **TspA has a toxic C-terminal domain with membrane depolarizing activity that is**
171 **neutralized by TsaI**

172 Sequence analysis of TspA indicates that homologues are found across the *Staphylococci*
173 (including *S. argenteus*, *S. epidermidis* and *S. lugdunensis*), in *Listeria* species and
174 Enterococci, but does not provide clues about potential function. However, analysis of TspA

175 using modelling programs predicts strong structural similarity to colicin Ia (Fig 3A), a
176 bacteriocidal protein produced by some strains of *Escherichia coli*. Colicin Ia has an
177 amphipathic domain at its C-terminus that inserts into the cytoplasmic membrane from the
178 extracellular side to form a voltage-gated channel[29-31]. Some limited structural similarity was
179 also predicted with the Type III secretion translocator protein YopB which undergoes
180 conformational changes to forms pores in host cell membranes[32].

181 To investigate the function of TspA, DNA encoding full length TspA or the C-terminal domain
182 alone ($TspA_{CT}$) was cloned into a tightly-regulatable vector for expression in *E. coli*. Fig 3C
183 shows that production of TspA or $TspA_{CT}$ did not affect *E. coli* survival. However, colicin Ia
184 shows a sidedness for channel formation because it requires a transmembrane voltage for full
185 insertion[33]. We therefore targeted $TspA_{CT}$ to the periplasm of *E. coli* by fusing to a Tat signal
186 peptide[34, 35]. Fig 3C shows that this construct was toxic, and that toxicity was relieved when
187 the Tat pathway was inactivated (Fig 3C), consistent with the C-terminal domain of TspA
188 exerting toxic activity from the periplasmic side of the membrane.

189 Bacterially-produced toxins, particularly those that target other bacteria, are often co-
190 expressed with immunity proteins that protect the producing cell from self-intoxication. For
191 example, protection from colicin Ia toxicity is mediated by the membrane-bound Iia immunity
192 protein[36]. TspA is genetically linked to a repeat region of ten genes encoding predicted
193 polytopic membrane proteins with DUF443 domains (Fig 3B). Topological analysis of these
194 proteins predicts the presence of five transmembrane domains with an N_{out}-C_{in} configuration.
195 Consistent with this, western blot analysis confirmed that a C-terminally HA-tagged variant of
196 SAOUHSC_00585, which is encoded directly adjacent to TspA, localized to the membrane of
197 *S. aureus* (Fig 3D). To determine whether SAOUHSC_00585 offers protection against the
198 toxicity of the TspA C-terminal domain, we co-produced the AmiAss-$TspA_{CT}$ fusion alongside
199 SAOUHSC_00585 in *E. coli*. Fig 3C shows that co-production of SAOUHSC_00585 offered
200 protection of *E. coli,* particularly when it was constitutively expressed from the pSUPROM
201 plasmid. SAOUHSC_00585 was subsequently renamed TsaI (TspA Immunity protein, Fig 3E).

202 Pore-forming proteins are widely used as toxins to target either prokaryotic or eukaryotic
203 cells[37, 38]. To assess whether TspA has pore/channel forming activity we investigated whether
204 the production of AmiAss-TspA$_{CT}$ in *E. coli* dissipated the membrane potential. Initially we used
205 the BacLight assay which is based on the dye 3,3′-diethyloxacarbocyanine iodide DiOC$_2$(3)
206 that exhibits green florescence in dilute solution but a red shift following membrane potential-
207 driven accumulation in the bacterial cytosol. After sorting of *E. coli* by flow cytometry, the
208 majority of cells harboring the empty vector exhibited red fluorescence, which shifted to green
209 following treatment with the uncoupler carbonyl cyanide 3-chlorophenylhydrazone (CCCP). A
210 similar shift in fluorescence was also observed when *E. coli* produced the AmiAss-TspA$_{CT}$
211 fusion (Fig 4A), indicative of loss of membrane potential. Co-production of TsaI offered some
212 protection from AmiAss-TspA$_{CT}$-induced depolarization (Fig 4A). We conclude that the C-
213 terminal domain of TspA has membrane depolarizing activity.

214 Membrane depolarization may arise from the formation of ion-selective channels or larger,
215 non-selective pores. To further investigate the mechanism of membrane depolarization we
216 used single-cell microscopy that combines the voltage-sensitive dye DiSC$_3$(5) with the
217 membrane-impermeable nucleic acid stain Sytox Green[39]. *E. coli* cells incubated with
218 Polymyxin B, which produces large ion-permeable pores in the *E. coli* cell envelope[40], showed
219 strong labelling with Sytox Green, indicative of permeabilisation, coupled with very low
220 DiSC$_3$(5) fluorescence (Fig 4B-D). By contrast, cells harboring the empty vector had high
221 DiSC$_3$(5) fluorescence that was unaffected by supplementation with the inducer L-arabinose,
222 and did not stain with Sytox Green. Cells expressing the AmiAss-TspA$_{CT}$ fusion following
223 incubation with arabinose rapidly depolarized, as evidenced by the marked reduction in
224 DiSC$_3$(5) fluorescence, but did not detectably stain with Sytox Green, even after prolonged
225 periods of incubation (Fig 4B-D, *SI Appendix*, Fig S3). Therefore, it appears that TspA acts by
226 triggering membrane depolarization but does so by forming ion channels rather than larger,
227 nonselective pores in the *E. coli* inner membrane. Again, co-production of TsaI significantly

228 protected cells from AmiAss-TspA$_{CT}$-induced depolarization, confirming that it acts as an
229 immunity protein (Fig 4B-D).

230 Bacterial channel-forming toxins have been reported that have either bacteriocidal[41] or
231 bacteriostatic[42] activity. To determine whether the C-terminal domain of TspA was
232 bacteriocidal or bacteriostatic, the growth of *E. coli* producing AmiAss-TspA$_{CT}$ was monitored.
233 It was observed that upon production of AmiAss-TspA$_{CT,}$ *E. coli* ceased to grow (Fig 4E),
234 however quantification of the colony forming units (cfu) indicated that the cells did not lose
235 viability (Fig 4F), pointing to a bacteriostatic action of TspA. We conclude that the C-terminal
236 domain of TspA is a channel-forming toxin with bacteriostatic activity, that is neutralized by
237 the action of TsaI.

238

239 **A zebrafish model for *S. aureus* infection and T7SS activity**

240 We next probed whether TspA was important for *S. aureus* virulence, initially through the
241 development of an immunocompetent murine model of *S. aureus* pneumonia. Previous
242 reports have indicated that 2-4 x 10^8 cfu of strain Newman was a suitable infectious dose, and
243 that bacterial proliferation in lung tissue could be observed after 24 hours[43]. We found that at
244 a dose of 8 x 10^7 – 2 x 10^8 of strain RN6390, the mice were asymptomatic and had almost
245 completely cleared the bacteria from lung tissue after 48 hours, whereas a dose of 8 x 10^8 –
246 2 x 10^9 was lethal to all mice within 12 hours. At a dose of 3 x 10^8, the mice developed
247 symptoms which resolved within 12 hours, and therefore using this dosage we sought to test
248 whether there was a difference in bacterial proliferation and dissemination dependent on the
249 T7SS. However, after 24 hours of infection with 3 x 10^8 cfu of RN6390 or a cognate Δ*essC*
250 strain, counts recovered from the lungs and livers of mice infected with the Δ*essC* strain were
251 not significantly different than those from mice infected with the wild type (*SI Appendix*, Fig
252 S4).

253 Given that there are likely to be roles for the T7SS in bacterial competition as well as direct
254 interaction with the host, we next developed a model where these two potentially confounding
255 factors could be investigated. The zebrafish (*Danio rerio*), a widely used vertebrate model for
256 development, has recently been adapted to study bacterial infection by human pathogens[44].
257 The hindbrain ventricle offers a sterile compartment that can be used to follow bacterial
258 interactions *in vivo*[45]. We first assessed the utility of this infection model by testing the effect
259 of dose and temperature on survival for *S. aureus* inoculated into the hindbrain ventricle of
260 zebrafish larvae 3 days post fertilisation (dpf; *SI Appendix*, Fig S5A). Clear dose-dependent
261 zebrafish mortality was observed, with ~90% of zebrafish surviving a low dose of *S. aureus*
262 infection (7 x 10^3 cfu) whereas only ~55% survived a higher dose (2 x 10^4 cfu; *SI Appendix*,
263 Fig S5B). Although 28.5°C is the optimum temperature for zebrafish larvae development, *S.*
264 *aureus* has a temperature optimum of 30 - 37°C for growth. In agreement with this, we
265 observed significantly increased zebrafish mortality at 33°C (relative to 28.5°C) at high dose
266 infection (*SI Appendix*, Fig S5B).

267 We next assessed whether there was a role for the T7SS in zebrafish mortality. For these
268 experiments, larvae at 3 dpf were inoculated in the hindbrain ventricle with 2 x 10^4 cfu of
269 RN6390 or an isogenic strain, RN6390 Δ*ess*, lacking all 12 genes (*esxA* through *esaG*) at the
270 *ess* locus[3], and incubated at 33°C. We routinely observed that zebrafish mortality was
271 significantly reduced, at both 24 and 48 hr post inoculation (hpi), for zebrafish infected with
272 the RN6390 Δ*ess* strain compared to the wild type (*SI Appendix*, Fig S5C; Fig 5A,C). In
273 agreement, total bacterial counts of infected zebrafish revealed that following an initial period
274 of six hours where both strains replicated in a similar manner, there was a significant decrease
275 in recovery of the Δ*ess* strain compared to the wild type after 9 hours (*SI Appendix*, Fig S5D;
276 Fig 5B,D), suggesting that bacteria lacking the T7SS are more rapidly cleared *in vivo*. We also
277 tested a second *S. aureus* strain, COL, in this assay. COL was only weakly virulent at 24 hpi,
278 but at high dose substantial mortality was seen after 48 hr (*SI Appendix*, Fig S6A). As before,
279 zebrafish mortality was at least in part dependent on a functional T7SS (*SI Appendix*, Fig

280 S6B), although we observed no difference in bacterial burden between the wild type and
281 Δ*essC* strain at the timepoints sampled (*SI Appendix*, Fig S6C). We conclude that the T7SS
282 plays a role in virulence of *S. aureus* in this zebrafish infection model.

283 In addition to TspA, a second T7SS secreted toxin, EsaD (also called EssD[9, 46]), a nuclease,
284 has been identified in some *S. aureus* strains. EsaD was shown to inhibit growth of a
285 competitor *S. aureus* strain *in vitro*[6], but has also been directly implicated in virulence through
286 modulation of cytokine responses and abscess formation[9, 46]. We therefore determined
287 whether TspA or EsaD was required for virulence in the zebrafish infection model. Infection of
288 larvae with strain RN6390 lacking TspA resulted in levels of mortality intermediate between
289 the wild type and Δ*ess* strain (Fig 5A), and a significantly reduced bacterial burden relative to
290 the wild type strain at 9 hpi (Fig 5B). By contrast, no difference was observed in either zebrafish
291 mortality (Fig 5C) or bacterial burden (Fig 5D) between infection with RN6390 and an isogenic
292 *esaD* mutant, indicating no detectable role of EsaD in virulence. Taken together, we conclude
293 that zebrafish infection can be used to investigate the role of T7SS effectors *in vivo*, and that
294 TspA (but not EsaD) contributes to T7SS-mediated bacterial replication *in vivo*.

295 Previous studies have shown that the T7SS of *S. aureus* is involved in modulating the murine
296 host immune response[9, 46]. To test whether altered immune responses mediate the increased
297 clearance of the Δ*ess* and Δ*tspA* deletion strains at 9 hpi, we investigated the role of the T7SS
298 in the zebrafish larval cytokine response during *S. aureus* infection *in vivo* (*SI Appendix*, Fig
299 S7). The expression of two host pro-inflammatory markers interleukin 8 (*cxcl8)* and interleukin
300 1 beta (*il-1b*) were quantified using qRT-PCR in larvae infected with 2 x 10^4 cfu of RN6390
301 wild type, Δ*ess*, Δ*tspA* and Δ*esaD* strains. In comparison to PBS injected larvae, *S. aureus*
302 infection caused a robust increase in both *cxcl8* and *il-1b* expression at 6 hpi (when the
303 bacterial burden among strains was similar; *SI Appendix*, Fig S7). However, no significant
304 difference in gene expression was observed among larvae infected with wild type and any of
305 the three deletion strains (Δ*ess*, Δ*tspA* and Δ*esaD*; *SI Appendix*, Fig S7).

306 Neutrophils represent the first line of defence against *S. aureus* infection[47] and the recently
307 discovered substrate of EssC variant 2 strains, named EsxX, has been implicated in neutrophil
308 lysis, therefore contributing to evasion of the host immune system[48]. By contrast, the T7SS of
309 *Mycobacterium tuberculosis* (ESX-1) is associated with manipulation of the inflammatory
310 response during infection allowing for bacterial replication in macrophages[49-52]. To investigate
311 whether the *S. aureus* T7SS modulates interaction with leukocytes, we analysed the
312 recruitment of immune cells to the hindbrain using two transgenic lines in which dsRed is
313 expressed specifically in neutrophils (Tg(*lyz*::dsRed)) or mCherry is expressed specifically in
314 macrophages (Tg(*mpeg*::Gal4-FF)^{gl25}/Tg(*UAS-E1b*::*nfsB*.mCherry)^{c264}, herein
315 Tg(*mpeg1*::G/U::mCherry)). Zebrafish larvae were infected with RN6390 wild type, Δ*ess* and
316 Δ*tspA* strains in the hindbrain ventricle at 3 dpf and imaged under a fluorescent
317 stereomicroscope at 0, 3 and 6 hpi in order to monitor neutrophil (*SI Appendix*, Fig S8A+B)
318 and macrophage (*SI Appendix*, Fig S8C+D) behavior. In zebrafish larvae infected with *S.*
319 *aureus*, a significant increase in neutrophil recruitment to the hindbrain ventricle was detected
320 in comparison to PBS-injected larvae at both 3 and 6 hpi (*SI Appendix*, Fig S8B). However,
321 no difference in neutrophil recruitment to the Δ*ess* and Δ*tspA* strains relative to wild type was
322 detected at any of the time points tested (*SI Appendix*, Fig S8B). Similar to the neutrophil
323 recruitment experiments, a significant increase in macrophage recruitment to the site of *S.*
324 *aureus* infection was observed when compared to PBS injected larvae at 3 hpi (*SI Appendix*,
325 Fig S8D). However, there was no significant difference in macrophage recruitment among the
326 wild type and T7SS mutant strains (*SI Appendix*, Fig S8D).

327

328 **T7SS dependent bacterial competition *in vivo***

329 Although TspA is required for optimal *S. aureus* virulence in the zebrafish model, the observed
330 toxicity when heterologously produced in *E. coli* coupled with the presence of immunity genes
331 encoded downstream of *tspA* strongly suggested that secreted TspA may also have

332 antibacterial activity. Previously, to observe antibacterial activity of the nuclease EsaD in
333 laboratory growth media required the toxin to be overproduced from a multicopy plasmid[6].
334 However, zebrafish larvae have recently been adapted to study bacterial predator-prey
335 interactions[45], and we reasoned that since the T7SS was active in our zebrafish infection
336 model it may also provide a suitable experimental system to investigate the impact of T7-
337 mediated bacterial competition *in vivo*.

338 In these experiments we used COL as the attacker strain and RN6360 and its derivatives as
339 the target; it should be noted that these strains produce the same TspA and EsaD isoforms
340 as well as similar suites of immunity proteins. COL was co-inoculated into the hindbrain
341 ventricle, at a 1:1 ratio, with either RN6390 or an isogenic strain lacking all potential immunity
342 proteins for EsaD and TspA (FRU1; RN6390 Δ*saouhsc00268-00278*, Δ*saouhsc00585-*
343 *00602*). A significant reduction in recovery of the target strain lacking immunity genes was
344 observed compared to the isogenic parental strain at 15 hr post infection (Fig 6A). Conversely,
345 there was significantly greater zebrafish mortality at 24 hr after co-inoculation of COL with the
346 wild type RN6390 than the immunity mutant strain (Fig 6B). Since COL is almost completely
347 avirulent at this time-point (*SI Appendix*, Fig S6) we infer that mortality arises from RN6390,
348 and as the wild type strain survives better than the immunity deletion strain when co-inoculated
349 with COL, this accounts for the greater zebrafish mortality.

350 To confirm that reduced growth of the RN6390 immunity mutant strain was dependent upon a
351 functional T7SS in the attacking strain, we repeated the co-inoculation experiments using a
352 T7 mutant strain of COL (COL Δ*essC*). The RN6390 immunity mutant strain showed
353 significantly higher recovery after 15 hours in the presence of the COL T7 mutant strain than
354 wild type COL (Fig 6C) and accordingly this was linked with reduced zebrafish survival (Fig
355 6D). Collectively, these data highlight the utility of zebrafish for investigating *S. aureus*
356 competition *in vivo*, and demonstrate that bacterial competition and zebrafish mortality is
357 dependent on a functional T7SS in the attacking strain (COL). This is outlined in the schematic
358 (Fig 6E). Conversely, the ability of the prey strain (RN6390) to survive T7-dependent killing is

359 dependent upon the immunity proteins against EsaD and TspA, because when these are not
360 present, fewer bacteria are recovered.

361 Finally, we investigated which of the EsaD and TspA toxins was responsible for inter-strain
362 competition by using variants of COL deleted for either *tspA* or *esaD* as the attacking strain. It
363 was seen that in the absence of either TspA (Fig 7A) or EsaD (Fig 7C) there was a significant
364 increase in recovery of the RN6390 Δ*saouhsc00268-00278*, Δ*saouhsc00585-00602* prey
365 strain, indicating that each of these toxins has activity against the target strain. However, there
366 was a more pronounced increase in zebrafish mortality when the attacker strain lacked *esaD*
367 than *tspA* (compare Figs 7B and D), suggesting that EsaD has the more potent antibacterial
368 activity in these conditions.

369 **Discussion**

370 Here we have taken an unbiased approach to discover substrates of the T7SS in *S. aureus*
371 RN6390, identifying the LXG-domain protein, TspA. TspA localizes to the cell envelope and
372 has a toxic C-terminal domain that has membrane-depolarizing activity. While all other
373 previously-identified T7 substrates are encoded at the *ess* locus and are associated with
374 specific *essC* subtypes[21, 48], TspA is encoded elsewhere on the genome, and is conserved
375 across all *S. aureus* strains. This suggests TspA plays a key role in *S. aureus*, and indeed we
376 show using a zebrafish infection model that it contributes to T7SS-mediated bacterial
377 replication *in vivo*.

378 Pore- and channel-forming toxins are key virulence factors produced by many pathogenic
379 bacteria[53], that can act both extracellularly to form pores in eukaryotic cells, like some bacterial
380 hemolysins[54], or intracellularly for example by altering permeability of the phagosome, like the
381 pore-forming toxin Listeriolysin-O, or the Type III secretion system effector VopQ[55, 56]. It should
382 be noted that the T7SS of strain USA300 has been shown to play a role in release of *S. aureus*
383 during intracellular infection[57], however RN6390 is only poorly invasive in bronchial epithelial
384 cell lines, and intracellular survival and bacterial release is independent of the T7SS (data not
385 shown). The *S. aureus* T7SS has been strongly linked with modulating the host innate immune
386 response[9, 45]. However, we did not observe any significant difference between wild type and
387 T7SS mutant strains in modulating cytokine expression and phagocyte recruitment in
388 zebrafish larvae. Although the precise mechanism by which the T7SS and TspA interacts with
389 host cells remains to be determined, we hypothesise that the T7SS plays a role after
390 phagocytosis by immune cells to influence intracellular survival. Future work using high
391 resolution single cell microscopy would allow for individual *S. aureus* cells, as well as their
392 interactions with neutrophils and/or macrophages, to be tracked *in vivo*.

393 Sequence alignments indicate that the C-terminal domain of TspA is polymorphic across *S.*
394 *aureus* strains (Fig S9) and structural modelling of TspA suggests homology to colicin Ia.

395 Colicin Ia is a toxin that forms voltage-gated ion channels in the plasma membrane of sensitive
396 *E. coli* strains. The formation of these channels results in lysis of target bacteria[30, 41].
397 Heterologous expression of the C-terminal predicted channel-forming domain of TspA was
398 shown to dissipate the membrane potential of *E. coli* when it was targeted to the periplasm,
399 probably through formation of an ion channel. Unlike Colicin Ia, however, heterologous
400 production of the TspA toxin domain was associated with a bacteriostatic rather than a
401 bacteriocidal activity. Colicins and pyocins are also examples of polymorphic toxins[38] and the
402 producing cells are generally protected from colicin-mediated killing by the presence of
403 immunity proteins[36]. A cluster of membrane proteins from the DUF443 domain family are
404 encoded downstream of *tspA*, and we show that at least one of these (SAOUHSC_00585;
405 TsaI) acts as an immunity protein to TspA by protecting *E. coli* from TspA-induced membrane
406 potential depletion.

407 Polymorphic toxins are frequently deployed to attack competitor bacteria in polymicrobial
408 communities[37], and there is growing evidence that a key role of the T7SS in some bacteria is
409 to mediate inter- and intra-species competition[6,7]. In addition to TspA, many commonly-studied
410 strains of *S. aureus*, including RN6390 and COL also secrete a nuclease toxin, EsaD[6]. We
411 adapted our zebrafish larval infection model to assess the role of the T7SS and the secreted
412 toxins TspA and EsaD in intra-species competition. We observed that strain COL was able to
413 outcompete RN6390 in a T7SS-dependent manner in these experiments, provided that
414 RN6390 was lacking immunity proteins to TspA and EsaD. Experiments with individual COL
415 attacker strains deleted for either *tspA* or *esaD* showed that each of the toxins contributed to
416 the competitiveness of COL in these assays. As *S. aureus* is a natural coloniser of human
417 nares and can also exist in polymicrobial communities in the lungs of cystic fibrosis patients,
418 we suggest that secreted T7 toxins including TspA allow *S. aureus* to establish its niche by
419 outcompeting other bacteria. Indeed, the observation that the T7SS gene cluster is highly
420 upregulated in the airways of a cystic fibrosis patient[5] would be consistent with this hypothesis.

421 LXG domain proteins appear to form a large substrate family of the firmicutes T7SS. Three
422 LXG domain proteins of *Streptococcus intermedius* have been shown to mediate contact-
423 dependent inhibition[7], and the association of TspA with the *S. aureus* cell envelope would also
424 imply that toxicity is contact-dependent. The LXG domain is predicted to form an extended
425 helical hairpin, which could potentially span the cell wall, displaying the toxin domain close to
426 the surface. How any of these toxin domains reach their targets in the prey cell is not clear.
427 One possibility is that the toxin domain is taken up into the target cell upon interaction with a
428 surface receptor, as observed for the Type V-dependent contact inhibition systems in Gram-
429 negative bacteria[58, 59]. During this process the CdiA protein, which also has a C-terminal toxin
430 domain, is proteolyzed, releasing the toxin to interact with its cellular target[60]. Further work
431 would be required to decipher the mechanism/s by which LXG toxins access target cells and
432 whether the toxin domains undergo proteolysis to facilitate cellular entry.

433 In conclusion, channel forming toxin substrates have been associated with other protein
434 secretion systems[42, 55, 56, 58], but this is the first to be functionally described for the T7SS. To
435 our knowledge it is only the second bacterial exotoxin identified to have a phenotype in both
436 bacterial competition and virulence assays, after VasX from *Vibrio cholerae*[61, 62].

437 **Materials and Methods**

438 **Bacterial strains, plasmids and growth conditions.** Construction of strains and plasmids,
439 and growth conditions are described in *SI Materials and Methods*. Plasmids and strains used
440 in this study are given in *SI Appendix*, Tables S2 and S3.

441

442 **Mass spectrometry data analysis and label-free quantitation.** Preparation of *S. aureus*
443 culture supernatants for proteomic analysis is detailed in *SI Materials and Methods*. Sample
444 preparation and mass spectrometry analysis was performed similar to previously described
445 work[63-66] and detailed methods are described in *SI Materials and Methods*.

446

447 **Cell fractionation and western blotting.** Preparation of *S. aureus* cell and supernatant
448 samples for western blotting, and subcellular fractionation of *S. aureus* into cell wall,
449 membrane and cytoplasmic fractions were as described previously[3]. Preparation of urea-
450 washed membrane fractions was adapted from Keller *et al.*[67]. Briefly, broken cell suspensions
451 were thoroughly mixed with a final concentration of 4M urea and incubated for 20 minutes at
452 room temperature. Membranes were harvested by ultracentrifugation (227 000 x *g*, 30 min).
453 The supernatant was retained as the urea-treated cytoplasmic fraction and the membrane
454 pellet resuspended in 1 x PBS, 0.5 % Triton X-100. For spheroplast preparation, the method
455 of Gotz *et al.*[68] was adapted. Briefly, strains were cultured as described above, cells were
456 harvested at OD_{600} of 2.0 and resuspended in Buffer A (0.7M sucrose, 20mM maleate, 20mM
457 $MgCl_2$, pH 6.5). Lysostaphin and lysozyme were added at 20 µg/ml and 2 mg/ml final
458 concentration, respectively, and cells incubated at 37°C for 1 hour. Cell debris was pelleted
459 by centrifugation (2,500 x *g* for 8 min) and the resulting supernatant centrifuged at 16,000 x *g*
460 for 10 min to pellet the spheroplasts. Spheroplasts were resuspended in Buffer A and treated
461 with increasing concentrations of Proteinase K on ice for 30 mins. 0.5 mM
462 phenylmethylsulfonyl fluoride was added to terminate the reaction and samples mixed with 4x
463 Nu PAGE LDS sample buffer and boiled for 10 min prior to further analysis. Western blotting

464 was performed according to standard protocols using the following antibody dilutions α-EsxA
465 [3] 1:2500; α-EsxC[3] 1:2000, α-EssB[3] 1:10000, α-TrxA[69] 1:25000, α-SrtA (Abcam, catalogue
466 number ab13959) 1:3000, α-HA (HRP-conjugate, Sigma catalogue number H6533) α-Myc
467 (HRP-conjugate, Invitrogen catalogue number R951-25) 1:5000, and goat anti Rabbit IgG
468 HRP conjugate (Bio-Rad, catalogue number 170-6515) 1:10000.
469
470 **Bacterial membrane potential detection.** To assess bacterial membrane potential, the
471 method of Miyata *et al.*[70] was adapted, using the BacLight bacterial membrane potential kit
472 (Invitrogen). Detailed methods to assess both bacterial membrane potential and
473 permeabilization are described in *SI Materials and Methods*.
474
475 **Zebrafish Infection.** Wild-type (WT, AB strain) or transgenic Tg(*lyz*::dsRed)^{nz50} [71] zebrafish
476 were used for all experiments. Embryos were obtained from naturally spawning zebrafish, and
477 maintained at 28.5°C until 3 days post fertilisation (dpf) in embryo medium (0.5x E2 medium
478 supplemented with 0.3 g/ml methylene blue)[72]. For injections, larvae were anesthetized with
479 200 µg/ml tricaine (Sigma-Aldrich) in embryo medium. Hindbrain ventricle infections were
480 carried out at 3 dpf and incubated at 33°C unless specified otherwise. Bacteria were
481 subcultured following overnight growth until they reached OD_{600} of 0.6. For injection of larvae,
482 bacteria were recovered by centrifugation, washed and resuspended in 1x PBS, 0.1% phenol
483 red, 1% polyvinylpyrrolidone to the required cfu/ml. Anaesthetized larvae were microinjected
484 in the hindbrain ventricle (HBV) with 1–2 nL of bacterial suspension. At the indicated times,
485 larvae were sacrificed in tricaine, lysed with 200 µL of 0.4% Triton X-100 and homogenized
486 mechanically. Larval homogenates were serially diluted and plated onto TSB agar. Only larvae
487 having survived the infection were included for enumeration of colony forming units (cfu). For
488 zebrafish virulence assays all *S. aureus* strains were chromosomally tagged with GFP which
489 included RN6390 wild type, and isogenic Δ*ess*, Δ*tspA* and Δ*esaD* strains. For *in vivo*
490 competition experiments, COL (attacker) strains were chromosomally-tagged with mCherry

491 and RN6390 (target) strains with GFP. Attacker and target strains were subcultured, harvested
492 and resuspended in PBS as above. Attacker and target strains were mixed at a 1:1 ratio and
493 injected in the hindbrain ventricle, with 1-2 nL of bacterial suspension. Larvae were sacrificed
494 at 15 hpi or 24 hpi, serially diluted and plated on TSB agar, and attacker and target strains
495 were enumerated by fluorescence (GFP and mCherry). Quantitative reverse transcription
496 PCR and *S. aureus* - leukocyte microscopy methods are described in *SI Materials and*
497 *Methods*.
498

499 **Acknowledgements**

500 This study was supported the Wellcome Trust [through Early Postdoctoral Training Fellowship
501 for Clinician Scientists WT099084MA to JDC, Investigator Award 110183/Z/15/Z to TP and
502 Institutional Strategic Support Fund 105606/Z/14/Z to the University of Dundee], the UK
503 Biotechnology and Biological Sciences Research Council [grants BB/H007571/1 and
504 EASTBIO DTP1 grant ref BB/J01446X/1], The Microbiology Society (through a Research Visit
505 Grant awarded to FRU) and a China Scholarship Council PhD studentship (to ZC). MT was
506 funded by the Medical Research Council UK through grant MC_UU_12016/5. Work in the SM
507 laboratory is supported by a European Research Council Consolidator Grant (772853 -
508 ENTRAPMENT), Wellcome Trust Senior Research Fellowship (206444/Z/17/Z) and the Lister
509 Institute of Preventive Medicine. We thank Professor Frank Sargent and Dr Sabine Grahl for
510 providing us with *E. coli* strain SG3000, Professor Jan-Maarten van Dijl (University of
511 Groningen) for the kind gift of anti-TrxA antiserum, and Drs Giuseppina Mariano, Sarah
512 Coulthurst, Vincenzo Torraca, and Melanie Blokesch for helpful discussion and advice.

513 **References**

514 1. Groschel, M.I., Sayes, F., Simeone, R., Majlessi, L. & Brosch, R. ESX secretion
515 systems: mycobacterial evolution to counter host immunity. *Nat Rev Microbiol* **14**, 677-
516 691 (2016).
517
518 2. Burts, M.L., Williams, W.A., DeBord, K. & Missiakas, D.M. EsxA and EsxB are secreted
519 by an ESAT-6-like system that is required for the pathogenesis of *Staphylococcus*
520 *aureus* infections. *Proc Natl Acad Sci USA* **102**, 1169-1174 (2005).
521
522 3. Kneuper, H. *et al.* Heterogeneity in ess transcriptional organization and variable
523 contribution of the Ess/Type VII protein secretion system to virulence across closely
524 related *Staphylocccus aureus* strains. *Mol Microbiol* **93**, 928-943 (2014).
525
526 4. Wang, Y. *et al.* Role of the ESAT-6 secretion system in virulence of the emerging
527 community-associated *Staphylococcus aureus* lineage ST398. *Sci Rep* **6**, 25163
528 (2016).
529
530 5. Windmuller, N. *et al.* Transcriptional adaptations during long-term persistence of
531 *Staphylococcus aureus* in the airways of a cystic fibrosis patient. *Int J Med Microbiol*
532 **305**, 38-46 (2015).
533
534 6. Cao, Z., Casabona, M.G., Kneuper, H., Chalmers, J.D. & Palmer, T. The type VII
535 secretion system of *Staphylococcus aureus* secretes a nuclease toxin that targets
536 competitor bacteria. *Nat Microbiol* **2**, 16183 (2016).
537
538 7. Whitney, J.C. *et al.* A broadly distributed toxin family mediates contact-dependent
539 antagonism between gram-positive bacteria. *eLife* **6,** e26938 (2017).
540
541 8. Klein, T.A., Pazos, M., Surette, M.G., Vollmer, W. & Whitney, J.C. Molecular Basis for
542 Immunity Protein Recognition of a Type VII Secretion System Exported Antibacterial
543 Toxin. *J Mol Biol* pii: S0022-2836(18)30594-1. doi: 10.1016/j.jmb.2018.08.027 (2018).
544
545 9. Ohr, R.J., Anderson, M., Shi, M., Schneewind, O. & Missiakas, D. EssD, a Nuclease
546 Effector of the *Staphylococcus aureus* ESS Pathway. *J Bacteriol* **199** e00528 (2017).
547
548 10. Rosenberg, O.S. *et al.* Substrates Control Multimerization and Activation of the Multi-
549 Domain ATPase Motor of Type VII Secretion. *Cell* **161**, 501-512 (2015).
550
551 11. Zoltner, M. *et al.* EssC: domain structures inform on the elusive translocation channel
552 in the Type VII secretion system. *Biochem J* **473**, 1941-1952 (2016).
553
554 12. Ramsdell, T.L., Huppert, L.A., Sysoeva, T.A., Fortune, S.M. & Burton, B.M. Linked
555 domain architectures allow for specialization of function in the FtsK/SpoIIIE ATPases
556 of ESX secretion systems. *J Mol Biol* **427**, 1119-1132 (2015).
557
558 13. Beckham, K.S. *et al.* Structure of the mycobacterial ESX-5 type VII secretion system
559 membrane complex by single-particle analysis. *Nat Microbiol* **2**, 17047 (2017).
560
561 14. Famelis *et al*. Architecture of the mycobacterial type VII secretion system. *Nature* **576,**
562 321-325 (2019).
563
564 15. Poweleit *et al*. The structure of the endogenous ESX-3 secretion system. *Elife* **8,** pii:
565 e52983 (2019).
566 .

16. Champion, P.A., Stanley, S.A., Champion, M.M., Brown, E.J. & Cox, J.S. C-terminal signal sequence promotes virulence factor secretion in *Mycobacterium tuberculosis*. *Science* **313**, 1632-1636 (2006).

17. Huppert *et al*. The ESX system in *Bacillus subtilis* mediates protein secretion. *PLoS One* **9,** e96267 (2014).

18. Baptista, C., Barreto, H.C. & São-José, C. High levels of DegU-P activate an Esat-6-like secretion system in *Bacillus subtilis*. *PLoS One* **8,** e67840 (2013).

19. Burts, M.L., DeDent, A.C. & Missiakas, D.M. EsaC substrate for the ESAT-6 secretion pathway and its role in persistent infections of *Staphylococcus aureus*. *Mol Microbiol* **69**, 736-746 (2008).

20. Anderson, M., Aly, K.A., Chen, Y.H. & Missiakas, D. Secretion of atypical protein substrates by the ESAT-6 secretion system of *Staphylococcus aureus*. *Mol Microbiol* **90**, 734-743 (2013).

21. Warne, B. *et al.* The Ess/Type VII secretion system of *Staphylococcus aureus* shows unexpected genetic diversity. *BMC Genomics* **17**, 222 (2016).

22. Anderson, M. *et al.* EssE Promotes *Staphylococcus aureus* ESS-Dependent Protein Secretion To Modify Host Immune Responses during Infection. *J Bacteriol* **199**, e00527 (2017).

23. Dreisbach, A. *et al.* Profiling the surfacome of *Staphylococcus aureus*. *Proteomics* **10**, 3082-3096 (2010).

24. Casabona, M.G. *et al.* Haem-iron plays a key role in the regulation of the Ess/type VII secretion system of *Staphylococcus aureus* RN6390. *Microbiology* **163**, 1839-1850 (2017).

25. Casabona, M.G. *et al.* Functional analysis of the EsaB component of the *Staphylococcus aureus* Type VII secretion system. *Microbiology* **163**, 1851–1863 (2017).

26. Jäger, F., Zoltner, M., Kneuper, H., Hunter, W.N. & Palmer, T. Membrane interactions and self-association of components of the Ess/Type VII secretion system of *Staphylococcus aureus*. *FEBS Letts* **590**, 349-357 (2016).

27. Zoltner, M., Fyfe, P.K., Palmer, T. & Hunter, W.N. Characterization of *Staphylococcus aureus* EssB, an integral membrane component of the Type VII secretion system: atomic resolution crystal structure of the cytoplasmic segment. *Biochem J* **449**, 469-477 (2013).

28. Zoltner, M. *et al.* The Architecture of EssB, an Integral Membrane Component of the Type VII Secretion System. *Structure* **21**, 595-603 (2013).

29. Wiener, M., Freymann, D., Ghosh, P. & Stroud, R.M. Crystal structure of colicin Ia. *Nature* **385**, 461-464 (1997).

30. Kienker, P.K., Qiu, X., Slatin, S.L., Finkelstein, A. & Jakes, K.S. Transmembrane insertion of the colicin Ia hydrophobic hairpin. *J Membr Biol* **157**, 27-37 (1997).

622 31. Kienker, P.K., Jakes, K.S., Blaustein, R.O., Miller, C. & Finkelstein, A. Sizing the
623 protein translocation pathway of colicin Ia channels. *J Gen Physiol* **122**, 161-176
624 (2003).
625
626 32. Dewoody, R.S., Merritt, P.M. & Marketon, M.M. Regulation of the *Yersinia* Type III
627 Secretion System: Traffic Control. *Front Cell Infect Microbiol* **3,** 4 (2013).
628
629
630 33. Qiu, X.Q., Jakes, K.S., Kienker, P.K., Finkelstein, A. & Slatin, S.L. Major
631 transmembrane movement associated with colicin Ia channel gating. *J Gen Physiol*
632 **107**, 313-328 (1996).
633
634 34. Ize, B., Stanley, N.R., Buchanan, G. & Palmer, T. Role of the *Escherichia coli* Tat
635 pathway in outer membrane integrity. *Mol Microbiol* **48**, 1183-1193 (2003).
636
637 35. Palmer, T. & Stansfeld, P.J. Targeting of proteins to the twin-arginine translocation
638 pathway. *Mol Microbiol,* **in press** doi: 10.1111/mmi.14461 (2020)
639
640 36. Weaver, C.A., Redborg, A.H. & Konisky, J. Plasmid-determined immunity of
641 *Escherichia coli* K-12 to colicin Ia Is mediated by a plasmid-encoded membrane
642 protein. *J Bacteriol* **148**, 817-828 (1981).
643
644 37. Seilie, E.S. & Bubeck Wardenburg, J. *Staphylococcus aureus* pore-forming toxins: The
645 interface of pathogen and host complexity. *Seminars in cell & developmental biology*
646 (2017).
647
648 38. Jamet, A. & Nassif, X. New players in the toxin field: polymorphic toxin systems in
649 bacteria. *MBio* **6**, e00285-00215 (2015).
650
651 39. Kepplinger, B. *et al.* Mode of Action and Heterologous Expression of the Natural
652 Product Antibiotic Vancoresmycin. *ACS Chem Biol* **13**, 207-214 (2018).
653
654 40. Daugelavicius, R., Bakiene, E. & Bamford, D.H. Stages of polymyxin B interaction with
655 the *Escherichia coli* cell envelope. *Antimicrob Agents Chemother* **44**, 2969-2978
656 (2000).
657
658 41. Jakes, K.S. & Finkelstein, A. The colicin Ia receptor, Cir, is also the translocator for
659 colicin Ia. *Mol Microbiol* **75,** 567-578 (2010).
660
661 42. Mariano, G. *et al*. A family of Type VI secretion system effector proteins that form ion-
662 selective pores. *Nat Commun* **10,** 5484. (2019).
663
664 43. Bubeck Wardenburg, J., Patel, R.J. & Schneewind, O. Surface proteins and exotoxins
665 are required for the pathogenesis of *Staphylococcus aureus* pneumonia. *Infect Immun*
666 **75**, 1040-1044 (2007).
667
668 44. Gomes M.C. & Mostowy, S. The Case for Modeling Human Infection in Zebrafish.
669 *Trends Microbiol* **28,** 10-18 (2020).
670
671 45. Willis, A.R. *et al.* Injections of Predatory Bacteria Work Alongside Host Immune Cells
672 to Treat *Shigella* Infection in Zebrafish Larvae. *Curr Biol* **26**, 3343-3351 (2016).
673
674 46. Anderson, M., Chen, Y.H., Butler, E.K. & Missiakas, D.M. EsaD, a Secretion Factor for
675 the Ess Pathway in *Staphylococcus aureus*. *J Bacteriol* **193**, 1583-1589 (2011).
676

677 47. Guerra, F.E., Borgogna, T.R., Patel, D.M., Sward, E.W. & Voyich, J.M. Epic Immune
678 Battles of History: Neutrophils vs. *Staphylococcus aureus*. *Front Cell Infect Microbiol*
679 **7,** 286 (2017)
680
681 48. Dai, Y. *et al.* A Novel ESAT-6 Secretion System-Secreted Protein EsxX of Community-
682 Associated *Staphylococcus aureus* Lineage ST398 Contributes to Immune Evasion
683 and Virulence. *Front Microbiol* **8**, 819 (2017).
684
685 49. Stanley, S.A., Raghavan, S., Hwang, W.W. & Cox, J.S. Acute infection and
686 macrophage subversion by *Mycobacterium tuberculosis* require a specialized
687 secretion system. *Proc Natl Acad Sci USA* **100,** 13001–13006 (2003).
688
689 50. MacGurn, J.A., Raghavan, S., Stanley, S.A., & Cox, J.S. A non-RD1 gene cluster is
690 required for Snm secretion in *Mycobacterium tuberculosis*. *Mol Microbiol* **57,** 1653–
691 1663 (2005).
692
693 51. Koo, I.C. *et al.* ESX-1-dependent cytolysis in lysosome secretion and inflammasome
694 activation during mycobacterial infection. *Cell Microbiol* **10,** 1866–1878 (2008).
695
696 52. Carlsson, F. *et al.* Host-Detrimental role of Esx-1-Mediated Inflammasome Activation
697 in *Mycobacterial* infection. *PLoS Pathog* **6,** e1000895 (2010).
698
699 53. Dal Peraro, M. & van der Goot, F.G. Pore-forming toxins: ancient, but never really out
700 of fashion. *Nat Rev Microbiol* **14**, 77-92 (2016).
701
702 54. Gonzalez-Juarbe, N. *et al.* Pore-Forming Toxins Induce Macrophage Necroptosis
703 during Acute Bacterial Pneumonia. *PLoS Pathog* **11**, e1005337 (2015).
704
705 55. Hamon, M.A., Ribet, D., Stavru, F. & Cossart, P. Listeriolysin O: the Swiss army knife
706 of Listeria. *Trends Microbiol* **20**, 360-368 (2012).
707
708 56. Sreelatha, A. *et al.* Vibrio effector protein, VopQ, forms a lysosomal gated channel that
709 disrupts host ion homeostasis and autophagic flux. *Proc Natl Acad Sci USA* **110**,
710 11559-11564 (2013).
711
712 57. Korea, C.G. *et al.* Staphylococcal Esx proteins modulate apoptosis and release of
713 intracellular *Staphylococcus aureus* during infection in epithelial cells. *Infect Immun*
714 **82**, 4144-4153 (2014).
715
716 58. Jones, A.M., Low,D.A. & Hayes, C.S. Can't you hear me knocking: contact-dependent
717 competition and cooperation in bacteria. *Emerg Top Life Sci* **1,** 75–83 (2017).
718
719 59. Danka,E.S., Garcia, E.C. & Cotter, P.A. Are CDI Systems Multicolored, Facultative,
720 Helping Greenbeards? *Trends Microbiol* **25,** 391–401 (2017).
721
722 60. Webb, J.S. et al. Delivery of CdiA nuclease toxins into target cells during contact-
723 dependent growth inhibition. *PLoS One* **8,**e57609 (2013).
724
725 61. Miyata, S.T., Kitaoka, M., Brooks, T.M., McAuley, S.B. & Pukatzki, S. *Vibrio cholerae*
726 requires the type VI secretion system virulence factor VasX to kill *Dictyostelium*
727 *discoideum*. *Infect Immun* **79**, 2941-2949 (2011).
728
729 62. Dong, T.G., Ho, B.T., Yoder-Himes, D.R. & Mekalanos, J.J. Identification of T6SS-
730 dependent effector and immunity proteins by Tn-seq in *Vibrio cholerae*. *Proc Natl Acad*
731 *Sci USA* **110**, 2623-2628 (2013).

732 63. Fritsch, M.J. *et al.* Proteomic identification of novel secreted antibacterial toxins of the
733 *Serratia marcescens* type VI secretion system. *Mol Cell Proteomics* **12**, 2735-2749
734 (2013).
735
736 64. Hamilton, J.J. *et al.* A holin and an endopeptidase are essential for chitinolytic protein
737 secretion in *Serratia marcescens*. *J Cell Biol* **207**, 615-626 (2014).
738
739 65. Cianfanelli, F.R. *et al.* VgrG and PAAR Proteins Define Distinct Versions of a
740 Functional Type VI Secretion System. *PLoS Pathog* **12**, e1005735 (2016).
741
742 66. Trunk, K. *et al.* The type VI secretion system deploys antifungal effectors against
743 microbial competitors. *Nat Microbiol* **3**, 920-931 (2018).
744
745 67. Keller, R., de Keyzer, J., Driessen, A.J. & Palmer, T. Co-operation between different
746 targeting pathways during integration of a membrane protein. *J Cell Biol* **199**, 303-315
747 (2012).
748
749 68. Gotz, F., Ahrne, S. & Lindberg, M. Plasmid transfer and genetic recombination by
750 protoplast fusion in staphylococci. *J Bacteriol* **145**, 74-81 (1981).
751
752 69. Miller, M. *et al. Staphylococcal* PknB as the first prokaryotic representative of the
753 proline-directed kinases. *PLoS ONE* **5**, e9057 (2010).
754
755 70. Miyata, S.T., Unterweger, D., Rudko, S.P. & Pukatzki, S. Dual expression profile of
756 type VI secretion system immunity genes protects pandemic *Vibrio cholerae*. *PLoS*
757 *Pathog* **9**, e1003752 (2013).
758
759 71. Hall, C., Flores, M.V., Storm, T., Crosier, K. & Crosier, P. The zebrafish lysozyme C
760 promoter drives myeloid-specific expression in transgenic fish. *BMC Dev Biol* **7**, 42
761 (2007).
762
763 72. Westerfield, M. *The zebrafish book. A guide for the laboratory use of zebrafish (Danio*
764 *rerio).* 4th edn. University of Oregon: Eugene, 2000.
765
766
767
768

Identifier	**Protein name/description**	**Relative abundance WT/Δ*essC***	**P-value**	**Unique peptides**	**Sequence coverage [%]**
SAOUHSC_ 00267	EsxD (T7 secreted substrate)	113.6*	8.00×10^{-6}	4	47.6
SAOUHSC_ 00584	(TspA) Uncharacterized LXG domain protein	15.9	2.45×10^{-3}	16	44.3
SAOUHSC_ 00268	EsaD (T7 secreted nuclease)	15.8	1.64×10^{-3}	24	44.5
SAOUHSC_ 00389	Uncharacterized. Predicted superantigen-like protein	6.7*	0.00109	2	25.6
SAOUHSC_ 00257	EsxA (Secreted T7 core component)	4.6	0.00425	6	81.4
SAOUHSC_ 00406	Uncharacterized protein	3.0	0.00272	10	31.7
SAOUHSC_ 01342	Nuclease SbcCD subunit C	2.9	0.00291	7	9.7

SAOUHSC_ 01949	Intracellular serine protease, putative	2.6	0.00421	7	20.8
SAOUHSC_ 02028	PhiETA ORF57-like protein	2.4	5.21×10^{-3}	13	26.4
SAOUHSC_ 01191	50S ribosomal protein L28	2.3	0.00498	3	24.2
SAOUHSC_ 02695	Uncharacterized protein with DUF4467/cystatin-like domain	2.3	0.00337	5	31
SAOUHSC_ 01180	Uncharacterized protein	2.3	0.00286	26	73.2
SAOUHSC_ 00258	EsaA (membrane-bound T7 core component)	2.2	0.00397	71	59.4
SAOUHSC_ 02448	Uncharacterized protein with alpha/beta hydrolase fold	2.1	0.00353	17	59.2
SAOUHSC_ 02042	Phi Mu50B-like protein	2.1	0.00141	2	18.9
SAOUHSC_ 02027	SLT orf 129-like protein	2.1	1.22×10^{-3}	4	56
SAOUHSC_ 02883	Staphylococcal secretory antigen SsaA	2.0	0.00431	5	43.1

769
770 **Table 1.** Proteins present in the secretome of RN6390 at an abundance of greater than 2-
771 fold higher than the secretome of the isogenic ΔessC strain. A full list of all of the proteins
772 identified in this analysis is given in *SI Appendix*, Table S1. *not detected in the Δ*essC*
773 secretome.

774 **SI Materials and Methods**

775 **Bacterial strains, plasmids and growth conditions.** All strains and plasmids used in this
776 study are given in *SI Appendix*, Tables S2 and S3. *S. aureus* strain RN6390[1] and its Δ*essC*[2],
777 Δ*esaD*[3], Δ*SAOUHSC_00268-00278*[3] and Δ*ess* (Δ*esxA-esaG*)[2] derivatives along with strain
778 COL[4] have been described previously. An in-frame deletion of *tspA* (*SAOUHSC_00584*) in
779 RN6390 was constructed by allelic exchange using plasmid pIMAY (*SI Appendix*, Table S3)[4].
780 The upstream and downstream regions including the start codon and last six codons were
781 amplified from RN6390 genomic DNA using primers listed in *SI Appendix*, Table S4 and were
782 cloned into pIMAY and introduced onto the chromosome by recombination as described
783 previously[4]. For deletion of *tsaI* and its homologues, the upstream regions of
784 *SAOUHSC_00585* including its first four codons and the downstream *SAOUHSC_00602*
785 including its last four codons were amplified from RN6390 genomic DNA, cloned into pIMAY
786 and was introduced into strain RN6390 Δ*SAOUHSC_00268-00278* to generate strain FRU1
787 (as RN6390 Δ*SAOUHSC_00268-00278*, Δ*SAOUHSC_00585-00602*). For in frame deletion of
788 *esaD* (SACOL0281) and *tspA* (SACOL0643) in strain COL, constructs pIMAY-esaD[3] and
789 pIMAY-tspA were used, following the protocol of Monk *et al*.[5]. Derivatives of strains harboring
790 markerless *gfp* or *mCherry* chromosomal insertions were constructed according to de Jong *et*
791 *al*.[6] using plasmids pTH100 and pRN111, respectively. *E. coli* strain JM110 was used for
792 cloning purposes and MG1655[7] and its isogenic Δ*tatABCD* derivative SG3000[8] was used for
793 toxicity assays.
794 All oligonucleotides used in this study are listed in *SI Appendix*, Table S4, and RN6390
795 chromosomal DNA was used as template unless otherwise stated. Plasmid pRAB11-tspA-
796 myc encodes TspA with a C-terminal Myc tag in pRAB11[9] and was constructed following
797 amplification with primers tspA cmyc fw and tspA cmyc rv. Plasmid pRAB11-02448-ha
798 produces SAOUHSC_02448 with a C-terminal HA tag from vector pRAB11 and the encoding
799 gene was amplified using primers 02448 cha fw and 02448 cha rv. Plasmid pRAB11-00389-
800 ha codes for SAOUHSC_00389 with a C-terminal HA tag in pRAB11 and was constructed

801 following amplification with primers 00389 cha fw and 00389 cha rv. Plasmid pRAB11-00406-
802 myc encodes SAOUHSC_00406 with a C-terminal Myc tag in pRAB11 and was constructed
803 following amplification with primers 00406 cmyc fw and 00406 cmyc rv. In each case the
804 amplified gene is preceded by the *esxA* RBS (AGGAGGTTTCTAGTT), and were cloned as
805 *Kpn*I - *Sac*I fragments. Plasmid pRAB11-00585-myc encodes SAOUHSC_00585 with a C-
806 terminal HA tag in pRAB11 and was constructed following amplification with primers 00585
807 cha fw and 00585 cha rv, digestion with *Bgl*II and *Eco*RI and cloning into similarly cut pRAB11.
808 Plasmid pRMC2-ssaA-ha codes for SsaA with a C-terminal HA tag. It was constructed
809 following amplification of SsaA using primers pRMC2-ssaA-bglII-for and pRMC2- ssaA-HA-
810 rev-EcoRI, digestion with *Bgl*II and *Eco*RI and cloning into similarly cut pRMC2[10].
811 Plasmid pBAD18-tspA codes for the full length TspA. The encoding gene was amplified using
812 primers tspA fl fw and tspA fl rv, digested with *Xba*I and *Sal*I and subsequently cloned into
813 similarly cut pBAD18-Cm[11]. Plasmid pBAD18-tspA$_{CT}$ encodes for the last 251aa of TspA; the
814 encoding DNA was amplified using primers tspA cp fw and tspA fl rv, digested with *Xba*I and
815 *Sal*I and cloned into similarly cut pBAD18-Cm. Plasmid pBAD18-AmiAss-tspA$_{CT}$ codes for the
816 *E. coli* AmiA signal sequence fused in-frame to the N-terminus of TspA$_{CT}$. This was
817 constructed following separate amplification of the DNA encoding the first 36 amino acids of
818 AmiA using primers AmiAss fw and AmiAss rv with *E. coli* MG1655 chromosomal DNA as
819 template digestion with *Nhe*I and *Kpn*I and cloning into similarly cut pBAD18-Cm. The TspA$_{CT}$
820 coding sequence was then amplified using tspA cp fw (which lacks a start codon) and tspA fl
821 rv, digested with *Xba*I and *Sal*I and cloned into similarly cut pBAD18-AmiAss. Plasmid
822 pBAD18-AmiAss-tspA$_{CT}$ + tsaI codes for the AmiAss-TspA$_{CT}$ fusion along with TsaI. The *tsaI*
823 (*saouhsc_00585*) gene was amplified using primers tsaI fw and tsaI rv, digested with *Sal*I and
824 *Sph*I and cloned into similarly cut pBAD18-AmiAss-tspA$_{CT}$.
825 Plasmid pSUPROM-TsaI produces TsaI constitutively from the *E. coli tat* promoter. The
826 encoding gene was amplified using primers pSU-TsaI fw and pSU-TsaI rv, digested with
827 *Bam*HI and *Xho*I and cloned into similarly-digested pSUPROM[12].

828 *S. aureus* strains were cultured in RPMI medium for proteomic analysis, as detailed below.
829 For all other experiments *S. aureus* strains were grown in TSB medium at 37°C with vigorous
830 agitation. Chloramphenicol was used 10 µg/ml final concentration for plasmid selection.
831 Anhydrotetracycline (ATC) was added to *S. aureus* cultures at 1 µg/ml during allelic gene
832 replacement. For induction of plasmid-encoded proteins, 500 ng/ml ATC was added to
833 cultures at OD_{600} of 0.4, and cells were harvested at OD_{600} of 2.0. *E. coli* was grown aerobically
834 in LB at 37°C, supplemented with ampicillin (100 µg/ml), kanamycin (50 µg/ml) or
835 chloramphenicol (25 µg/ml) where appropriate. D-glucose and L-arabinose were used to
836 control expression of cloned genes from the pBAD18-Cm vector[11]. For toxicity assays single
837 colonies of MG1655 freshly transformed with the appropriate pBAD18-Cm construct growing
838 on LB agar containing 0.2% D-glucose were picked and re-suspended in LB to an OD_{600} of
839 1.0. Serial dilutions to 10^{-5} were prepared and 5 µL of each spotted onto LB agar supplemented
840 with 0.2% D-glucose, 0.02% L-arabinose or 0.2% L-arabinose and incubated overnight at
841 37°C. For growth curve measurements, overnight cultures of MG1655 harboring pBAD18-Cm
842 constructs were sub-cultured to a starting OD_{600} of 0.1 (t=0) and incubated at 37°C and allowed
843 to reach an OD_{600} of 0.5 before supplementation with 0.2% L-arabinose. Optical density
844 readings at 600nm were taken for a 6 hour growth period, with readings collected every 2
845 hours. The number colony forming units was calculated at t=0 and every 2 hours post-
846 induction with L-arabinose. Serial dilutions to 10^{-6} were prepared and 100 µL of each plated
847 onto LB agar containing 25 µg/ml chloramphenicol and incubated overnight at 37°C.
848
849 **Preparation of culture supernatants for proteomic analysis.** *S. aureus* strains were grown
850 overnight in 2 mL TSB after which cells were harvested, washed three times with 10 mL of
851 RPMI medium, resuspended in 2 mL of RPMI and used to inoculate 200 mL RPMI in 2 L
852 baffled flasks. Cultures were grown at 37°C with vigorous agitation until an OD_{600} of 1.0 was
853 reached, after which cultures were cooled to 4°C, cells pelleted and supernatant proteins
854 precipitated with 6% trichloroacetic acid (TCA) on ice overnight. The precipitated protein
855 samples were harvested by centrifugation (15 min at 18000 *g*) re-suspended in 80% acetone

856 (-20°C) and washed twice with 80% acetone. Pellets were air dried at room temperature and
857 transferred to the mass-spectrometry facility for proteomic analysis.
858
859 **Mass spectrometry data analysis and label-free quantitation.** Sample preparation and
860 mass spectrometry analysis was performed similar to previously described work[13-16].
861 Precipitated proteins were re-dissolved in 1% sodium 3-[(2-methyl-2-undecyl-1,3-dioxolan-4-
862 yl)methoxy]-1-propanesulfonate (commercially available as RapiGest, Waters), 50 mM Tris-
863 HCl pH 8.0, 1 mM TCEP. Cysteines were alkylated by addition of 20 mM Iodoacetamide and
864 incubation for 20 min at 25°C in the dark and the reaction quenched by addition of 20 mM
865 DTT. Samples were diluted to 0.1% Rapigest with 50 mM Tris-HCl pH 8.0 and Trypsin
866 (sequencing grade, Promega) was added at a 1:50 ratio. Proteins were digested overnight at
867 37°C under constant shaking.
868 Samples from four biological replicates (0.5 µg of digest for the secretome analyses) were
869 injected in an interleaved manner onto a 2 cm x 100 µm trap column and separated on a 50
870 cm x 75 µm EasySpray Pepmap C18 reversed-phase column (Thermo Fisher Scientific) on a
871 Dionex 3000 Ultimate RSLC. Peptides were eluted by a linear 3-hour gradient of 95% A/5% B
872 to 35% B (A: H_2O, 0.1% Formic acid (FA); B: 80% ACN, 0.08% FA) at 300 nl/min into a LTQ
873 Orbitrap Velos (Thermo-Fisher Scientific). Data was acquired using a data-dependent "top 20"
874 method, dynamically choosing the most abundant precursor ions from the survey scan (400-
875 1600 Th, 60,000 resolution, AGC target value 10^6). Precursors above the threshold of 2000
876 counts were isolated within a 2 Th window and fragmented by CID in the LTQ Velos using
877 normalized collision energy of 35 and an activation time of 10 ms. Dynamic exclusion was
878 defined by a list size of 500 features and exclusion duration of 60 s. Lock mass was used and
879 set to 445.120025 for ions of polydimethylcyclosiloxane (PCM).
880 Label-free quantitation was performed using MaxQuant 1.5.7.4[17]. Data were searched against
881 the Uniprot database of *S. aureus* NCTC8325 (downloaded on 29.03.17) containing 2,889
882 sequences and a list of common contaminants in proteomics experiments using the following
883 settings: enzyme Trypsin/P, allowing for 2 missed cleavage, fixed modifications were

884 carbamidomethyl (C), variable modifications were set to Acetyl (Protein N-term), Deamidation
885 (NQ) and Oxidation (M). MS/MS tolerance was set to 0.5 Da, precursor tolerance was set to
886 6 ppm. Peptide and Protein FDR was set to 0.01, minimal peptide length was 7, and one
887 unique peptide was required. Re-quantify and retention time alignment (2 min) were enabled.
888 If no intensities were detected in one condition and the other condition had intensities in at
889 least in 3 out of 4 replicates, values were imputed in Perseus v1.5.1.1 using default
890 parameters[18]. A student's t-test (two-tailed, homoscedastic) was performed on the LFQ
891 intensities and only proteins with $p<0.05$ and a fold-change >2-fold were considered
892 significant.
893
894 **Data availability statement.** Raw mass spectrometry data that support the findings of this
895 study have been deposited to the ProteomeXchange Consortium via the PRIDE[19] partner
896 repository with the dataset identifier PXD011358. All other data supporting the findings of this
897 study are available within the paper and its supplementary information files.
898
899 **Bacterial membrane potential detection.** To assess bacterial membrane potential, the
900 method of Miyata *et al.*[20] was adapted, using the BacLight bacterial membrane potential kit
901 (Invitrogen). In brief, overnight cultures of *E. coli* MG1655 harboring pBAD18-Cm derivatives
902 were sub-cultured into LB medium containing appropriate antibiotics to an OD_{600} of 0.1 and
903 cultured aerobically to OD_{600} of 0.5, before supplementation with 0.2% L-arabinose. Cells were
904 cultured for a further hour then diluted to 1 x 10^6 cells per ml in sterile PBS, and a 1ml aliquot
905 of bacterial suspension was added to each flow cytometry tube. For the depolarized control,
906 25 µL of 500 µM carbonyl cyanide m-chlorophenyl hydrazone (CCCP), provided in the
907 BacLight bacterial membrane potential kit, was added. Next, 3 µL of 3mM $DiOC_2(3)$ was added
908 to each sample, which was mixed and incubated at room temperature for 30 minutes. Cells
909 were subsequently sorted using an LSRFortessa cell analyzer (BD Biosciences, San Jose,
910 CA). The $DiOC_2(3)$ dye was excited at 488 nm, with fluorescent emissions detected using
911 Alexa488 (Ex 488nm, Em 530/30 nm) and Alexa568 (Ex 561 nm, Em 610/20 nm). In total,

912 20000 events were collected for each sample, with forward- and side-scatter parameters used
913 to gate the bacteria. The forward scatter, side scatter, and fluorescence were collected with
914 logarithmic signal amplification. The gated populations were then analyzed with FlowJo
915 software by generating a dot plot of red versus green fluorescence.
916 To assess changes in membrane potential and permeabilization, the same *E. coli* strains were
917 grown as described above. An 'uninduced' sample of *E. coli* harboring each of pBAD18-Cm
918 (empty), pAmiAss-TspA$_{CT}$ and pAmiAss-TspA$_{CT}$-TsaI was collected and adjusted to OD_{600} of
919 0.2 before the addition of 2 μM $DiSC_3(5)$ and 200 nM Sytox Green. A permeabilized control
920 sample of cells harboring empty vector and containing 10 μg/ml Polymyxin B was also
921 prepared and supplemented with both dyes. All samples were then incubated at 37°C for 5
922 minutes before being analyzed by microscopy. To induce protein production from the pBAD18-
923 Cm vector, cell suspensions were adjusted to OD_{600} of 0.2 and supplemented with 0.2% L-
924 arabinose for the indicated period of time (10-60 min) before incubating with $DiSC_3(5)$ and
925 Sytox Green, as above. Imaging of $DiSC_3(5)$ and Sytox Green stained cells was carried out
926 Nikon Eclipse Ti equipped with Sutter Instrument Lambda LS light source, Nikon Plan Apo
927 100×/1.40 NA Oil Ph3 objective, and Photometrics Prime sCMOS, and Cy5 and GFP filters,
928 respectively. The images were captured using Metamorph 7.7 (Molecular Devices) and
929 analyzed using ImageJ. For the analysis, the phase contrast images acquired in parallel to the
930 fluorescence images were used to identify cells as regions of interest, for which average
931 $DiSC_3(5)$ and Sytox Green fluorescence intensity was measured from the corresponding
932 background-subtracted fluorescence images. Data was then plotted as a scatter plot for
933 $DiSC_3(5)$ and Sytox Green fluorescence with each point representing an individual cell.
934

935 **Mouse pneumonia model.** *S. aureus* RN6390 (WT) or the isogenic Δ*essC* strain were
936 subcultured at 1:100 dilution from an overnight culture into fresh TSB medium. Cells were
937 grown at 37°C with shaking until an OD_{600} of 0.5 was reached, before harvesting and washing
938 three times in 1x PBS. Cells were finally resuspended in 1 x PBS to 1.2 x 10^{10} cfu/ml. Female

939 10-12 week old C57/B6 J mice were purchased from Charles River U.K.. Mice were
940 acclimatized for a 10 day period prior to starting the experiment. Mice were randomized to
941 cages and treatment groups, and analyses were performed blind. Mice were anaesthetized
942 (gaseous isofluorane) and infected intranasally with 25 µL of the bacterial suspension to give
943 a final infected dose of 3 x 10^8 cfu per mouse. At 24 hours post infection the lungs and livers
944 were harvested and the bacterial load determined by plating serial dilutions of tissue
945 homogenates.
946

947 **Quantitative reverse transcription polymerase chain reaction (qRT-PCR).** For RNA was
948 harvested from 10 snap-frozen zebrafish larvae infected with *S. aureus* at 6 hpi using the
949 RNeasy Mini Kit (Qiagen) as per manufacturer's instructions. RNA was reverse transcribed
950 into cDNA using QuantiTect Reverse Transcription Kit (Qiagen) as per manufacturer's
951 instructions with 500 ng of RNA. Quantitative RT-PCR reactions were performed on four
952 biological replicates, each with two technical replicates. For qRT-PCR reactions, 50 ng of
953 cDNA was used per reaction with SYBR Green Reaction Mix (Thermo Fisher Scientific) on a
954 Rotor GeneQ (Qiagen) thermocycler. Oligonucleotides for *il-1b*, *cxcl8* and *eef1a1a* are listed
955 in *SI Appendix*, Table S4. Quantities of cDNA were normalised using the housekeeping gene
956 *eef1a1a* and the 2-ΔΔCT method was used for analysis[21].
957

958 **Imaging of *S. aureus* – leukocyte interactions *in vivo*.** To observe *S. aureus* – leukocyte
959 interactions, Tg(*lyz*::dsRed)^{nz50} and Tg(*mpeg1*::Gal4-FF)^{gl25}/Tg(*UAS-E1b*::*nfsB*.mCherry)^{c264}
960 zebrafish larvae were infected with *S. aureus* strains chromosomally labelled with GFP. To
961 follow neutrophil and macrophage recruitment, infected larvae were anaesthetised with 200
962 µg/ml Tricaine and the HBV imaged at 0, 3, and 6 hpi by fluorescence stereomicroscopy and
963 multiple position z stacks of up to 400 µm were acquired using a Leica M205FA
964 stereomicroscope with a 10x (NA 0.5) dry objective. Neutrophil and macrophage
965 quantifications were performed manually throughout the individual z stacks using Fiji – ImageJ

(ver 1.0).

Statistical analysis. For statistical analysis GraphPad Prism 6.0 software was used. In survival assays statistical analysis was done using a Log rank (Mantel-Cox) test. To analyse bacterial kinetics, CFU counts were Log10 transformed and the significance between two independent groups was determined by an unpaired *t* test. When more than two groups were compared, significance was determined by using one-way ANOVA with Sidak's comparison. Gene expression levels were quantified on Log2 data and significance was determined by using one-way ANOVA with Sidak's Multiple Comparison test. For leukocyte cell counts analysis (non-parametric data), significance between multiple selected groups was determined using Kruskal-Wallis test with Dunn's correction. Significance is indicated ns, non-significant, *, $p \leq 0.05$; **, $p \leq 0.01$; ***, $p \leq 0.001$; ****, $p \leq 0.0001$.

SI References

1. Novick, R.P. *et al.* Synthesis of staphylococcal virulence factors is controlled by a regulatory RNA molecule. *EMBO J* **12**, 3967-3975 (1993).

2. Kneuper, H. *et al.* Heterogeneity in ess transcriptional organization and variable contribution of the Ess/Type VII protein secretion system to virulence across closely related *Staphylocccus aureus* strains. *Mol Microbiol* **93**, 928-943 (2014).

3. Cao, Z., Casabona, M.G., Kneuper, H., Chalmers, J.D. & Palmer, T. The type VII secretion system of *Staphylococcus aureus* secretes a nuclease toxin that targets competitor bacteria. *Nat Microbiol* **2**, 16183 (2016).

4. Dyke, K.G., Jevons, M.P. & Parker, M.T. Penicillinase production and intrinsic resistance to penicillins in *Staphylococcus aureus*. *Lancet* **1**, 835-838 (1966).

5. Monk, I.R., Shah, I.M., Xu, M., Tan, M.W. & Foster, T.J. Transforming the untransformable: application of direct transformation to manipulate genetically *Staphylococcus aureus* and *Staphylococcus epidermidis*. *MBio* **3** e00277 (2012).

6. de Jong, N.W., van der Horst, T., van Strijp, J.A. & Nijland, R. Fluorescent reporters for markerless genomic integration in *Staphylococcus aureus*. *Sci Rep* **7**, 43889 (2017).

7. Blattner, F.R. *et al.* The complete genome sequence of *Escherichia coli* K-12. *Science* **277**, 1453-1462 (1997).

8. Grahl, S. Tat signal peptide recognition during protein maturation and export. doctoral degree thesis, University of Dundee, Dundee, 2011.

9. Helle, L. *et al.* Vectors for improved Tet repressor-dependent gradual gene induction or silencing in *Staphylococcus aureus*. *Microbiology* **157**, 3314-3323 (2011).

10. Corrigan, R.M. & Foster, T.J. An improved tetracycline-inducible expression vector for *Staphylococcus aureus*. *Plasmid* **61**, 126-129 (2009).

11. Guzman, L.M., Belin, D., Carson, M.J. & Beckwith, J. Tight regulation, modulation, and high-level expression by vectors containing the arabinose P_{BAD} promoter. *J Bacteriol* **177**, 4121-4130 (1995).

12. Jack, R.L. *et al.* Coordinating assembly and export of complex bacterial proteins. *EMBO J* **23**, 3962-3972 (2004).

13. Fritsch, M.J. *et al.* Proteomic identification of novel secreted antibacterial toxins of the *Serratia marcescens* type VI secretion system. *Mol Cell Proteomics* **12**, 2735-2749 (2013).

14. Hamilton, J.J. *et al.* A holin and an endopeptidase are essential for chitinolytic protein secretion in *Serratia marcescens*. *J Cell Biol* **207**, 615-626 (2014).

15. Cianfanelli, F.R. *et al.* VgrG and PAAR Proteins Define Distinct Versions of a Functional Type VI Secretion System. *PLoS Pathog* **12**, e1005735 (2016).

16. Trunk, K. *et al.* The type VI secretion system deploys antifungal effectors against microbial competitors. *Nat Microbiol* **3**, 920-931 (2018).

17. Cox, J. & Mann, M. MaxQuant enables high peptide identification rates, individualized p.p.b.-range mass accuracies and proteome-wide protein quantification. *Nat Biotechnol* **26**, 1367-1372 (2008).

18. Tyanova, S. *et al.* The Perseus computational platform for comprehensive analysis of (prote)omics data. *Nat. Methods* **13**, 731-740 (2016).

19. Vizcaino, J.A. *et al.* 2016 update of the PRIDE database and its related tools. *Nucleic Acids Res.* **44**, D447-456 (2016).

20. Miyata, S.T., Unterweger, D., Rudko, S.P. & Pukatzki, S. Dual expression profile of type VI secretion system immunity genes protects pandemic *Vibrio cholerae*. *PLoS Pathog* **9**, e1003752 (2013).

21. Livak, K.J. & Schmittgen, T.D. Analysis of relative gene expression data using real-time quantitative PCR and the 2-ΔΔCT method. *Methods* **25,** 402–408 (2001).

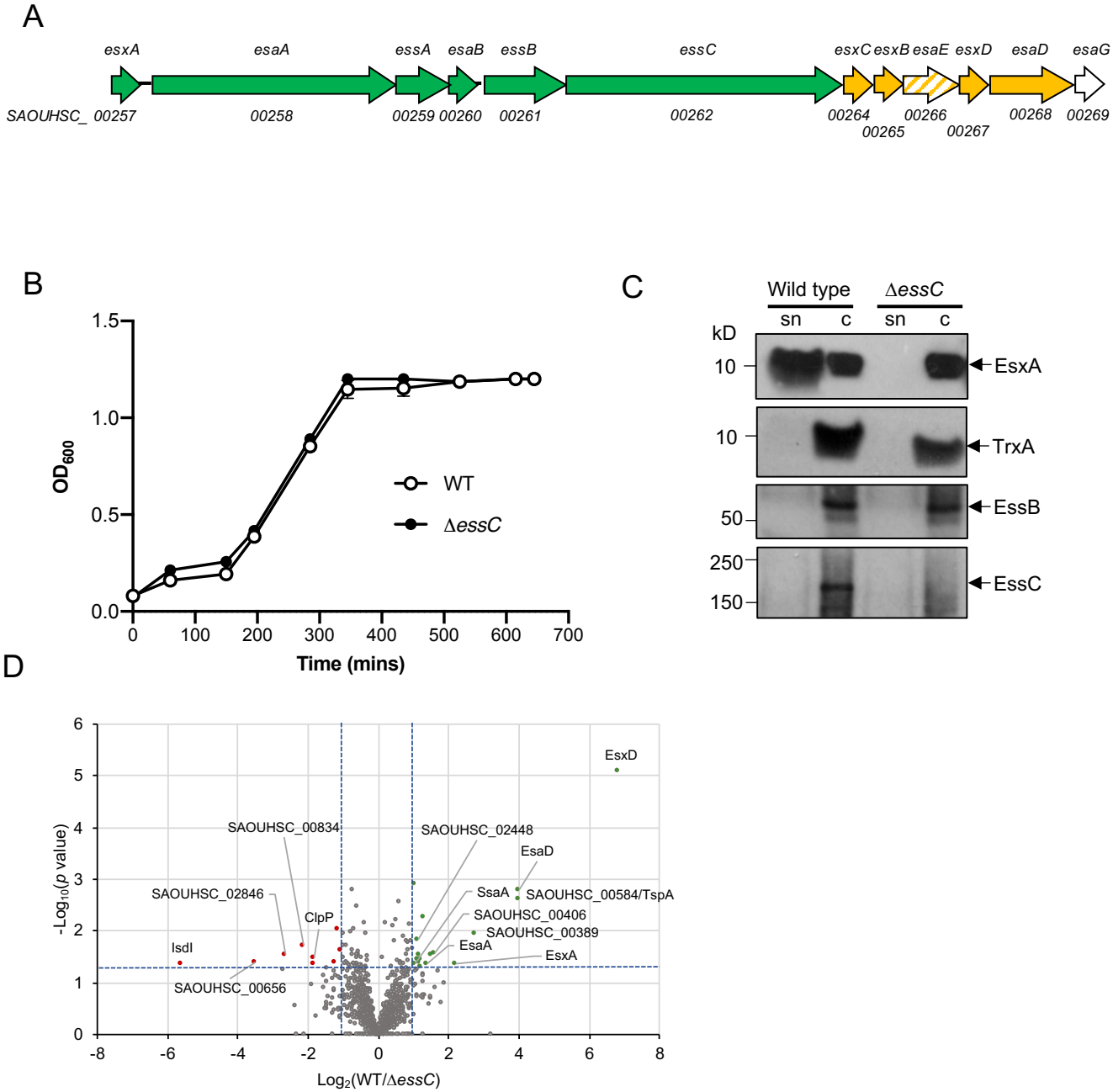

Figure 1. The *S. aureus* RN6390 T7 secretome. A. the *ess* locus in strain NCTC8325 (parent of RN6390). Genes for core components are shaded green, secreted substrates yellow, EsaE (which is co-secreted with EsaD) in hatched shading and the cytoplasmic antitoxin EsaG in white. B. Growth of RN6390 (WT) and the isogenic Δ*essC* strain in RPMI medium. Points show mean +/− SEM ($n = 3$ biological replicates). C. RN6390 (WT) and the Δ*essC* strain cultured in RPMI growth medium to OD_{600} = 1. Samples were separated into supernatant (sn) and cellular (c) fractions (12% bis-Tris gels) and immunoblotted with anti-EsxA, anti-EssB, anti-EssC or anti-TrxA (cytoplasmic protein) antisera. D. Volcano plot of the quantitative proteomic secretome analysis. Each spot represents an individual protein ranked according to its statistical *p*-value (y-axis) and relative abundance ratio (log_2 fold change). The blue dotted lines represent cut-offs for significance ($p<0.05$; log_2 fold-change>1).

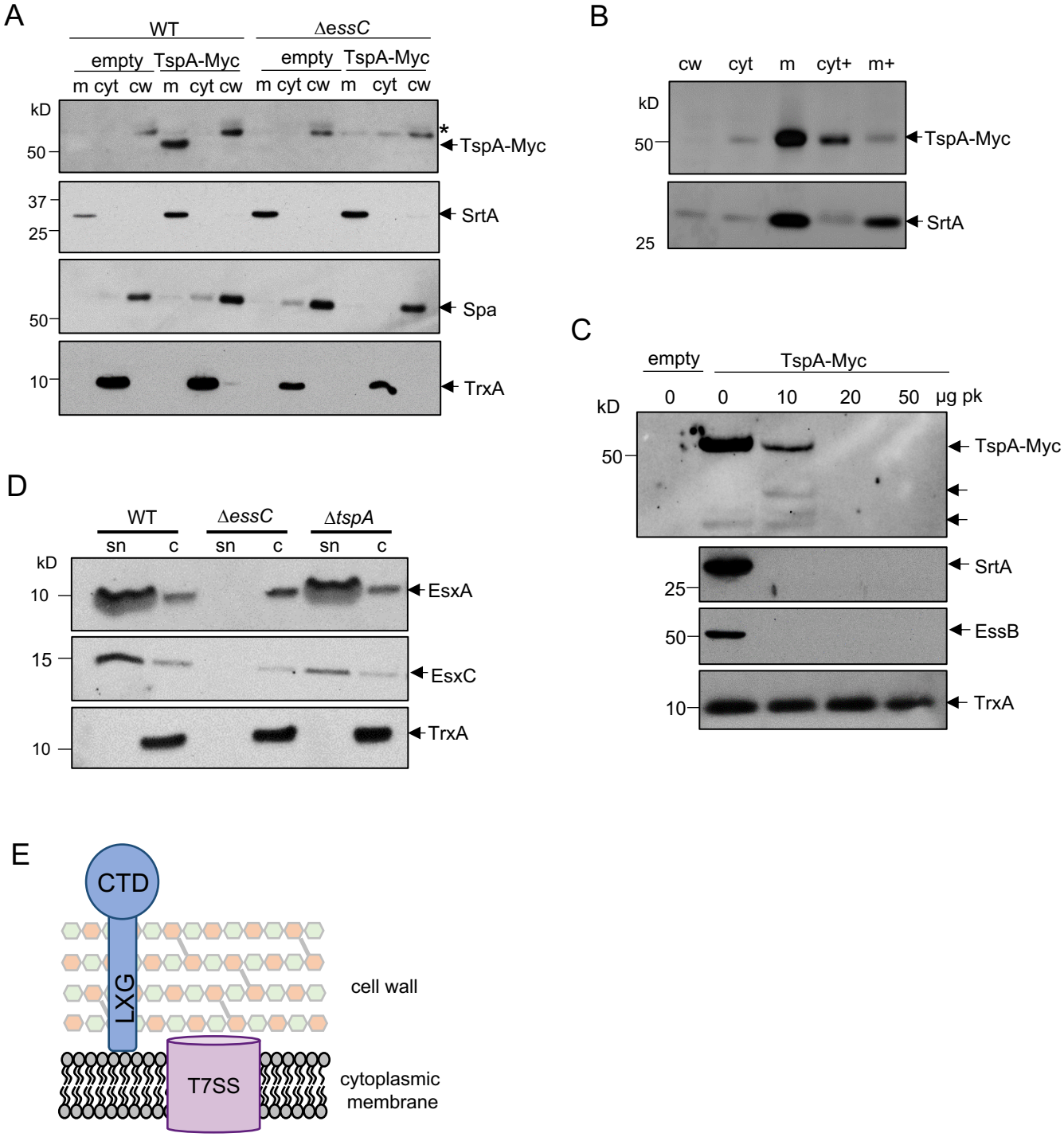

Figure 2. SAOUHSC_00584/TspA is an extracellular peripheral membrane protein. A. RN6390 (WT) and the Δ*essC* strain harbouring pRAB11 (empty) or pRAB11-TspA-Myc were cultured in TSB growth medium. Following induction of plasmid-encoded TspA-Myc production, cells were harvested and fractionated into cell wall (cw), membrane (m) and cytoplasmic (cyt) fractions. Samples were separated (12% bis-Tris gels) and immunoblotted with anti-Myc-HRP anti-TrxA (cytoplasmic protein), anti-Spa (cell wall) or anti-SrtA (membrane) antisera. * 'non-specific' cross-reacting band corresponding to Spa. B. Cell extracts from the RN6390 samples in (A) were incubated with 4M urea, membranes were isolated and the urea-treated cytoplasm (cyt+) and membranes (m+) were separated alongside the cell wall and untreated cytoplasm and membrane fractions on a 12% bis-tris gel and immunoblotted with anti-Myc and anti-SrtA antisera. C. Spheroplasts from strain RN6390 producing TspA-Myc were incubated with the indicated concentrations of Proteinase K (pk) at 4°C for 30 mins. A sample of spheroplasts from RN6390 containing pRAB11 (empty) is shown as a negative control. Samples were separated on a 12% bis-tris gel and immunoblotted using anti-Myc, anti-SrtA, anti-EssB and anti-TrxA antisera. D. *S. aureus* RN6390 or the isogenic Δ*essC* or Δ*tspA* strains were cultured in TSB medium and harvested at OD_{600} of 2. Supernatant (sn) and cellular (c) fractions (equivalent of 100 µl culture supernatant and 10 µl of cells adjusted to OD_{600} of 2.0) were separated on bis-Tris gels (15% acrylamide) and immunoblotted using anti-EsxA, EsxC or TrxA antisera. E. Model for organization of TspA in the *S. aureus* envelope. CTD – C-terminal (channel-forming) domain.

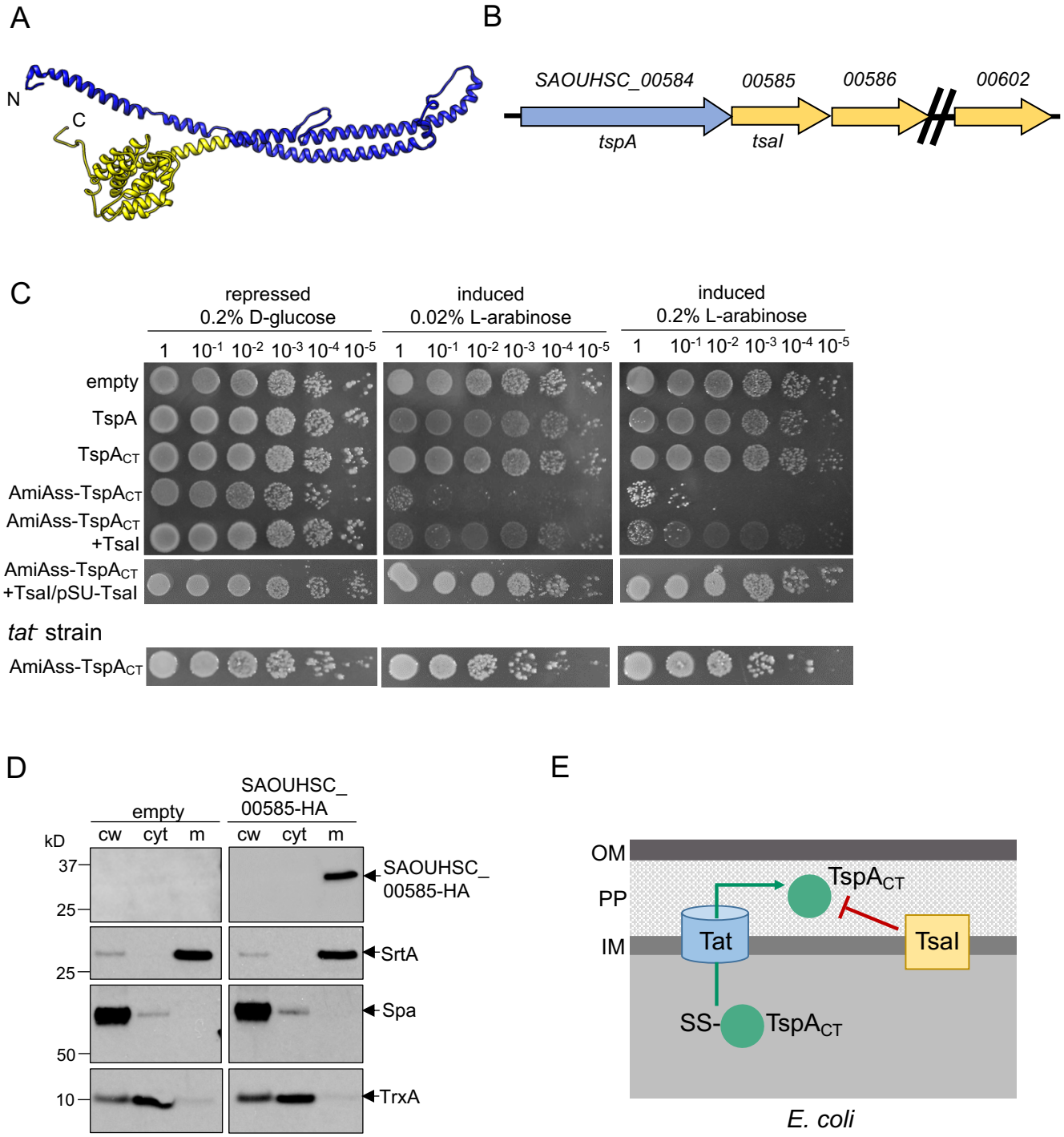

Figure 3. Directed export of TspA C-terminal domain to the periplasm of *E. coli* is toxic. A. Structural model for residues 9-416 of TspA generated using RaptorX (http://raptorx.uchicago.edu/), modelled on the colicin Ia structure [27]. The predicted channel-forming region is shown in yellow. B. The *tspA* locus. Genes coding for DUF443 proteins are shown in yellow. C. *E. coli* strain MG1655 harboring empty pBAD18-Cm or pBAD18-Cm encoding either full length TspA, the TspA C-terminal domain ($TspA_{CT}$), $TspA_{CT}$ with the AmiA signal sequence at its N-terminus (AmiAss-$TspA_{CT}$), AmiAss-$TspA_{CT}$ and TsaI (SAOUHSC_00585), AmiAss-$TspA_{CT}$/TsaI alongside an additional plasmid-encoded copy of TsaI (from Psu-TsaI) or strain SG3000 (as MG1655, Δ*tatABCD*) harboring pBAD18-AmiAss-$TspA_{CT}$ was serially diluted and spotted on LB plates containing either D-glucose or L-arabinose, as indicated. Plates were incubated at 37°C for 16 hours after which they were photographed. D. *S. aureus* cells harbouring pRAB11 (empty) and pRAB11-SAOUHSC_00585-HA were cultured in TSB medium and expression of SAOUHSC_00585-HA induced by addition of 500 ng/ml ATc when the cells reached OD_{600} of 0.4. The cells were then harvested at OD_{600} of 2. The cells were spun down and subsequently fractionated into cell wall (cw), membrane (m) and cytoplasmic (cyt) fractions. The fractionated samples were separated on bis-tris gels and immunoblotted using the anti-HA antibody, or control anti-sera raised to TrxA (cytoplasmic protein), protein A (SpA, cell wall) or sortase A (SrtA, membrane). E. Schematic representation of the toxicity experiments in Fig 3C, and the inhibition of $TspA_{CT}$ toxicity by the membrane-embedded immunity protein, TsaI. OM, outer membrane; PP, periplasm; IM, inner membrane.

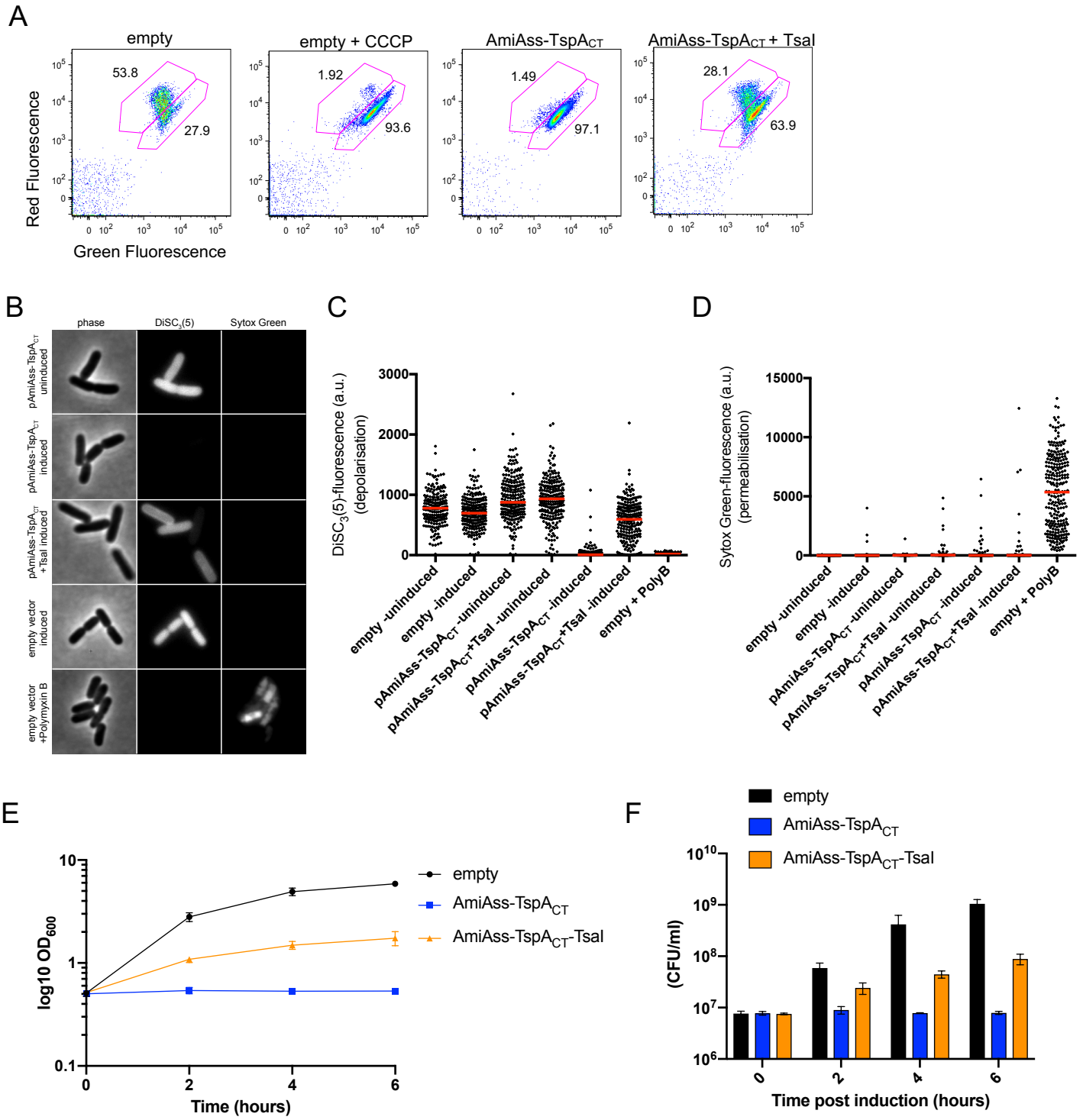

Figure 4. The C-terminal domain of TspA has bacteriostatic activity and disrupts the membrane potential. A. *E. coli* MG1655 harboring pBAD18-Cm (empty), or pBAD18-Cm encoding AmiAss-TspA$_{CT}$ or AmiAss-TspA$_{CT}$ / TsaI were grown in the presence of 0.2% L-arabinose for 1 hour at which point they diluted to 1 x 10^6 cells per ml and supplemented with 30 µM DiOC$_2$(3) for 30 mins. One sample of MG1655 harboring pBAD18 (empty) was also supplemented with 5 µM CCCP at the same time as DiOC$_2$(3) addition. Strains were analyzed by flow cytometry. B-D. The same strain and plasmid combinations as A were grown in the presence (induced) or absence (uninduced) of 0.2% L-arabinose for 30 minutes after which they were supplemented with DiSC$_3$(5) and Sytox Green and B. imaged by phase contrast and fluorescence microscopy. C+D. Fluorescence intensities of C. DiSC$_3$(5) and D. Sytox Green for each sample was quantified using image J. A control sample where Polymyxin B was added to the uninduced empty vector control for 5 minutes before supplemented with DiSC$_s$(5) and Sytox Green was included in each experiment. E+F. Growth of *E. coli* MG1655 harboring pBAD18-Cm (empty), or pBAD18-Cm encoding AmiAss-TspA$_{CT}$ or AmiAss-TspA$_{CT}$ / TsaI upon induction with 0.2% L-arabinose. LB medium was inoculated with an overnight culture of *E. coli* strain MG1655 harbouring the indicated constructs to a starting OD$_{600}$ of 0.1. Cells were incubated at 37°C and allowed to reach an OD$_{600}$ of 0.5 (indicated by time 0) before supplementing the growth medium with 0.2% L-arabinose (inducing conditions). The growth was monitored every 2 hours and the colony forming units at each time point was determined (F). Points and bars show mean +/− SEM (n = 3 biological replicates).

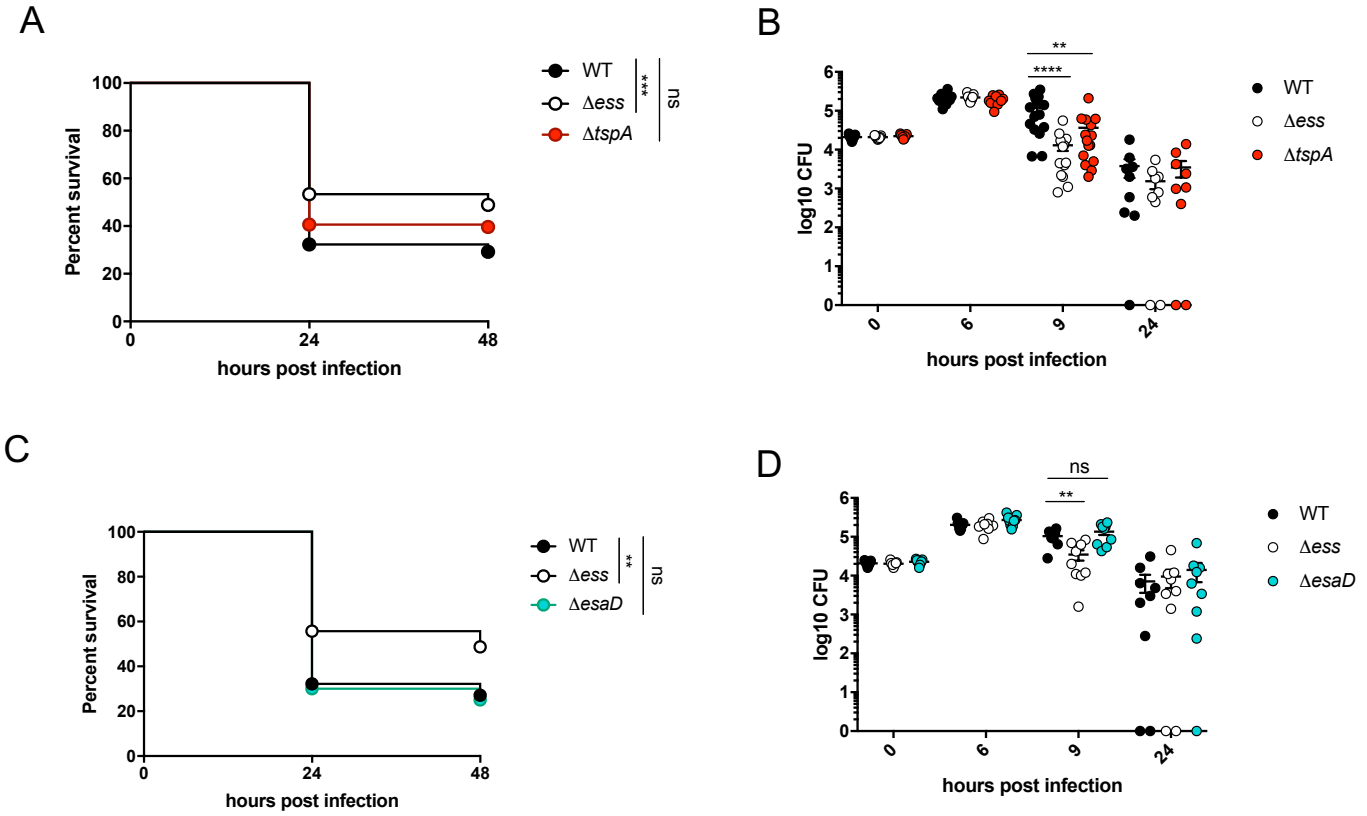

Figure 5. The T7SS contributes to virulence in a zebrafish infection model. A. Survival curves of 3 dpf zebrafish *lyz*:dsRed larvae infected in the hindbrain ventricle with RN6390-gfp (WT) or otherwise isogenic Δ*ess*-gfp or Δ*tspA*-gfp strains at a dose of ~2 x 10^4 cfu and incubated at 33°C for 48 hpi. Data are pooled from four independent experiments (*n*=25-51 larvae per experiment). Results were plotted as a Kaplan-Meier survival curve and the *p* value between conditions was determined by log-rank Mantel-Cox test. B. Enumeration of recovered bacteria at 0, 6, 9 or 24 hpi from zebrafish larvae infected with the same strains as A. Pooled data from 3 independent experiments. Circles represent individual larva, and only larvae that survived the infection were included. No significant differences observed between strains at 0, 6 or 24 hpi. Mean ± SEM also shown (horizontal bars). Significance testing was performed using a one-way ANOVA with Sidak's correction at each timepoint. C. Survival curves of 3 dpf zebrafish *lyz*:dsRed larvae infected in the hindbrain ventricle with RN6390-gfp (WT) or otherwise isogenic Δ*ess*-gfp, Δ*esaD*-gfp strains at a dose of ~2 x 10^4 cfu and incubated at 33°C for 48 hpi. Data are pooled from three independent experiments (*n*=26-32 larvae per experiment). Results are plotted as a Kaplan-Meier survival curve and the *p* value between conditions was determined by log-rank Mantel-Cox test. D. Enumeration of recovered bacteria at 0, 6, 9 or 24 hpi from zebrafish larvae infected with the strains as C. Pooled data from 3 independent experiments. Circles represent individual larva, and only larvae having survived the infection were included. No significant differences observed between strains at 0, 6 or 24 hpi. Mean ± SEM also shown (horizontal bars). Significance testing was performed using a one-way ANOVA with Sidak's correction at each timepoint. ***p*<0.01, *** *p*<0.001, **** *p*<0.0001, ns, not significant.

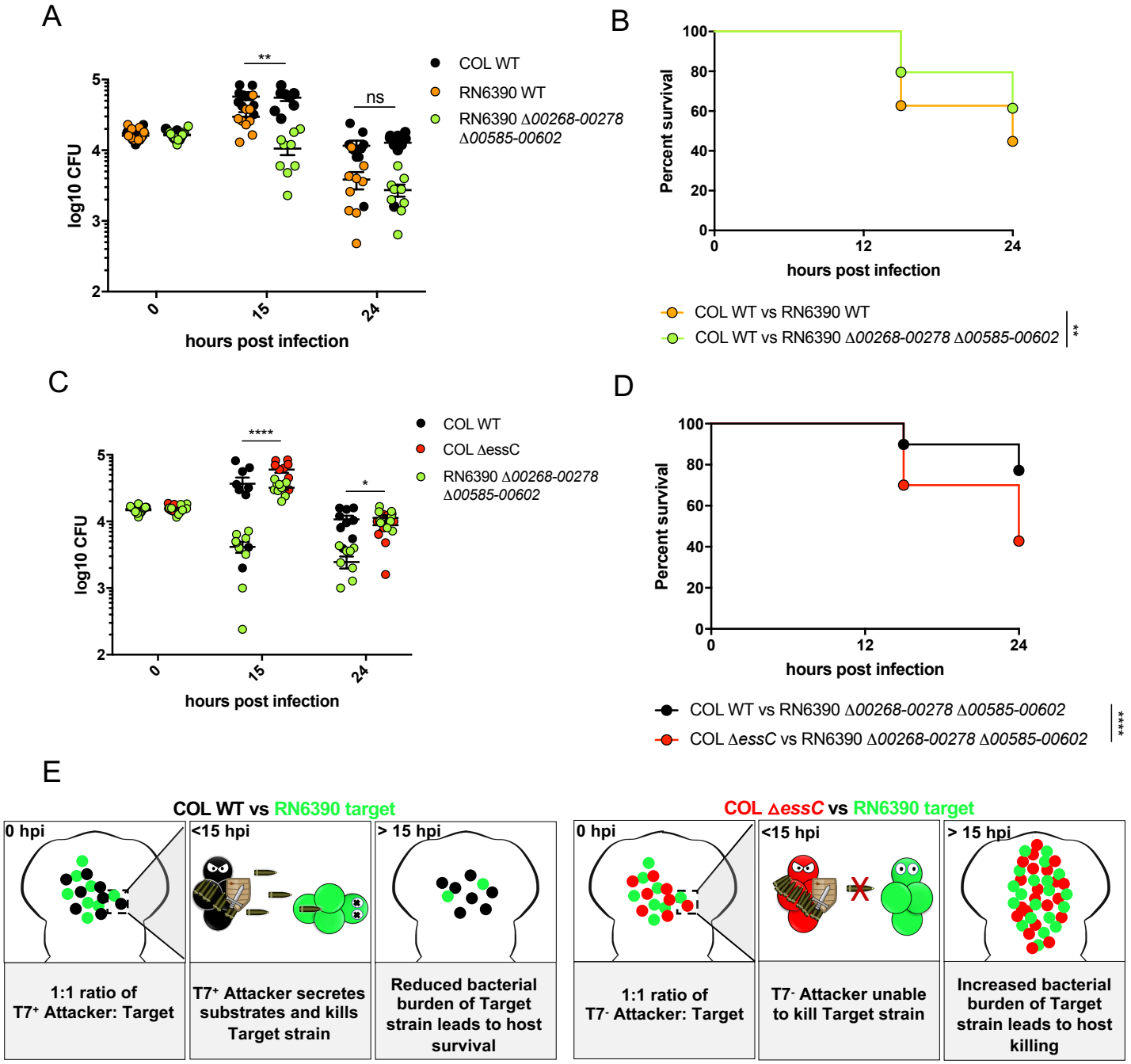

Figure 6. Development of an *in vivo* model to study bacterial competition. Wild type AB zebrafish larvae at 3 dpf were co-infected with a 1:1 mix of an attacker strain (either COL-mCherry (WT) or COL Δ*essC*-mCherry as indicated) and a target strain (either RN6390-gfp (WT) or RN6390 Δ*00268-278* Δ*00585-00602*-gfp, as indicated). A+C. Enumeration of recovered attacker and prey bacteria from zebrafish larvae at 0, 15 or 24 hpi. Pooled data from 3 independent experiments, Mean ± SEM also shown (horizontal bars). Significance testing performed by unpaired *t* test. B+D. Survival curves of zebrafish injected with the indicated strain pairs. Data are pooled from three independent experiments. Results are plotted as a Kaplan-Meier survival curve and the p value between conditions was determined by log-rank Mantel-Cox test. ** $p<0.01$, *** $p<0.001$, **** $p<0.0001$, ns, not significant. E. Model highlighting the role for the T7SS in competition *in vivo*.

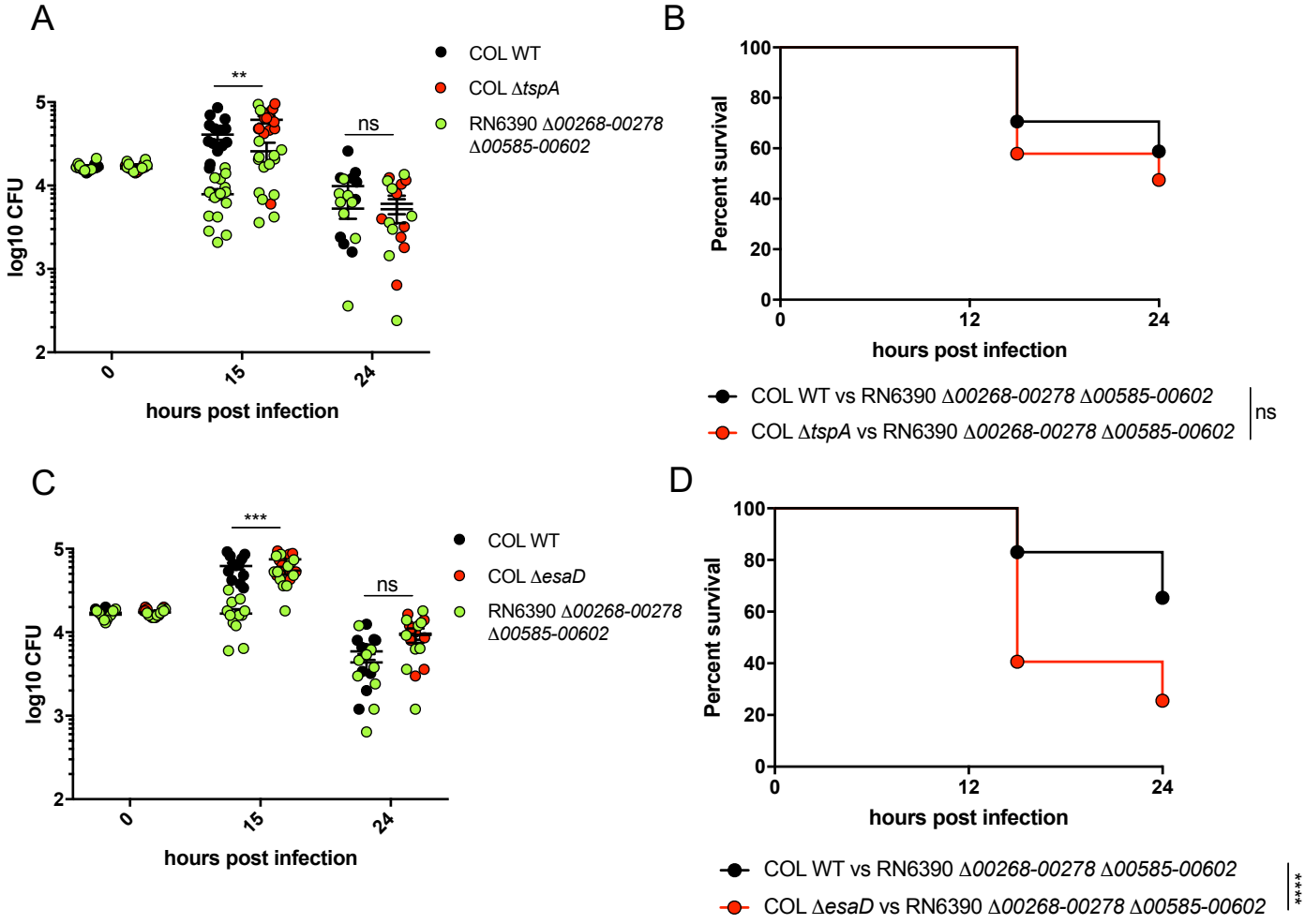

Figure 7. TspA and EsaD dependent bacterial competition *in vivo*. Wild type AB zebrafish larvae at 3 dpf were co-infected with a 1:1 mix of an attacker strain (either COL-mCherry (WT), COL Δ*tspA*-mCherry or COL Δ*esaD*-mCherry as indicated) and a target strain (RN6390 Δ*00268-278* Δ*00585-00602*-gfp). A+C. Enumeration of recovered attacker and prey bacteria from zebrafish larvae at 0, 15 or 24 hpi. Pooled data from 3 independent experiments, Mean ± SEM also shown (horizontal bars). Significance testing performed by unpaired *t* test. B +D. Survival curves of zebrafish injected with the indicated strain pairs. Data are pooled from three independent experiments. Results are plotted as a Kaplan-Meier survival curve and the *p* value between conditions was determined by log-rank Mantel-Cox test. ** $p<0.01$, *** $p<0.001$, **** $p<0.0001$, ns, not significant.

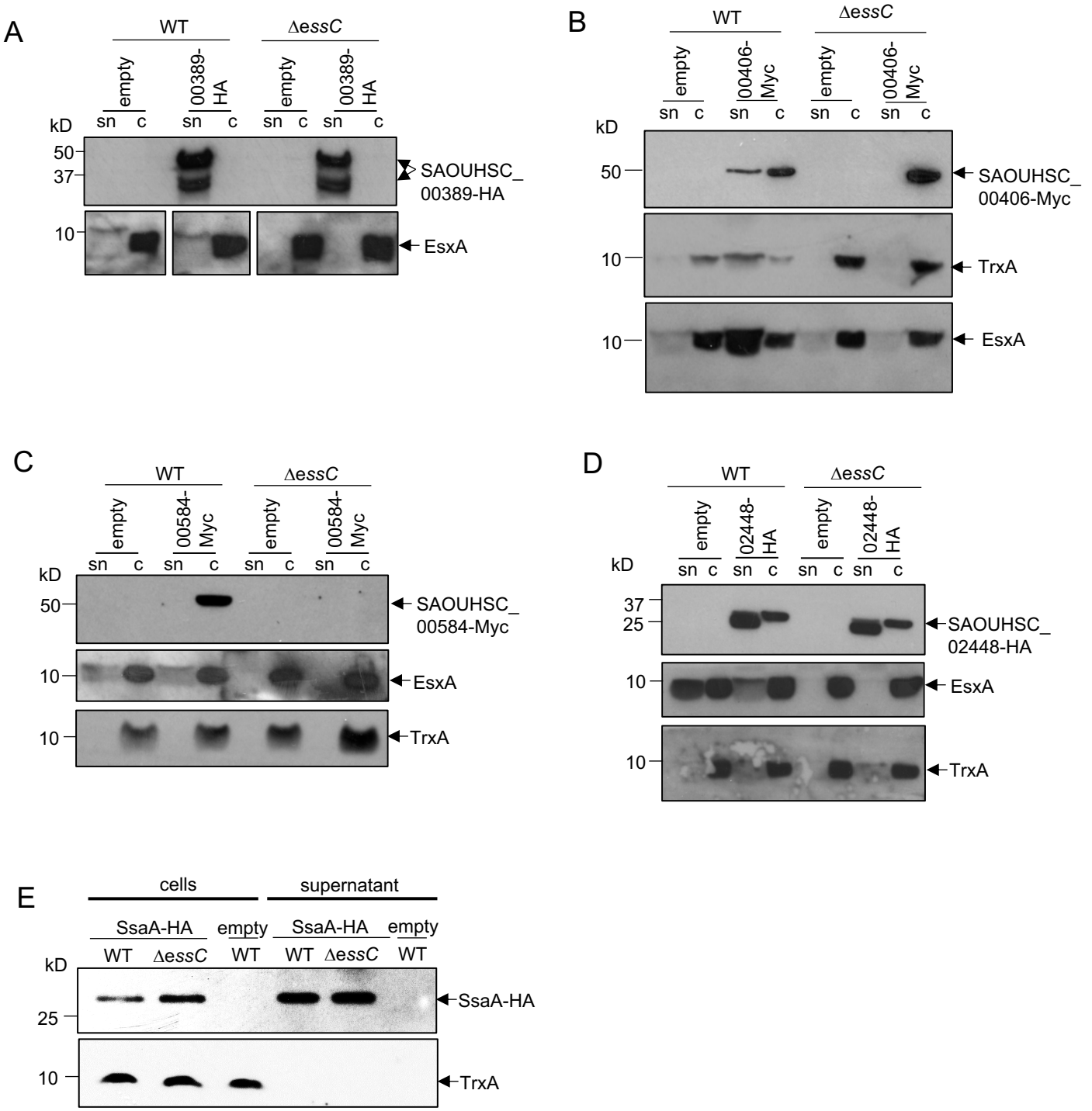

Figure S1. HA-tagged variants of SAOUHSC_00389, SAOUHSC_02448 and SsaA are not secreted by the T7SS. The wild type RN6390 and Δ*essC* mutant carrying A-D pRAB11 (empty) or pRAB11 encoding A. C-terminally HA-tagged SAOUHSC_00389; B. C-terminally Myc-tagged SAOUHSC_00406; C. C-terminally Myc-tagged tagged SAOUHSC_00584; or D. C-terminally HA-tagged SAOUHSC_02448, or E. pRMC2 (empty) or encoding C-terminally HA-tagged SsaA were cultured in TSB medium and supplemented with 200ng/ml ATc at OD_{600} of 0.5. When cultures reached OD_{600} of 2.0, samples were withdrawn and separated into culture supernatant (sn) and cellular (c) fractions. Samples were separated on 12% bis-Tris gels and immunoblotted with anti-HA, anti-Myc, anti-EsxA or anti-TrxA antibodies, as indicated.

MSIDMYLDRSRNQASSVGNLSQTMNSNYDALEKAITQFINDDALKGKAYTSAKQFFSTVLIPLSTSMK
TLSDLTKQACDNFVSRYTSEVDSISLKESELEEDIRSLSQQITRYENLNNNLKKHASDNQQAISSNQQ
IIRTLGQQKHELEEKLRKLREFNQKSPEIFKEVEEFQKIVQQGLTQAQNFWNFSTNQFNIPSGKELDW
AKASHEKYLKVAMGKIEHKAEKETLNKADFAVIKAYAKEHPEDDIPKSILKYINDNKDSIKRDIGLDI
TSTLLEQDGINASKFGVFINTAGGVKGPAGPNSFVEVKRTSGNVFIENGSKFAKGGKYLGKGVAGVGF
GIGMYDDLANDDKTFGEALSHNGMTLAAGSAGTAVGAGLATFVLGSNPVGWVILAGLAMSTVFALGTD
LIYQNNIFGLKDKVDWVGHKIDNSIDVVKKTTEKSMDSVGNAVSEAKNIISNHINPMKWAW

Figure S2. Peptide coverage of TspA from proteomic analysis. Regions of TspA coloured orange were detected by mass spectroscopy analysis.

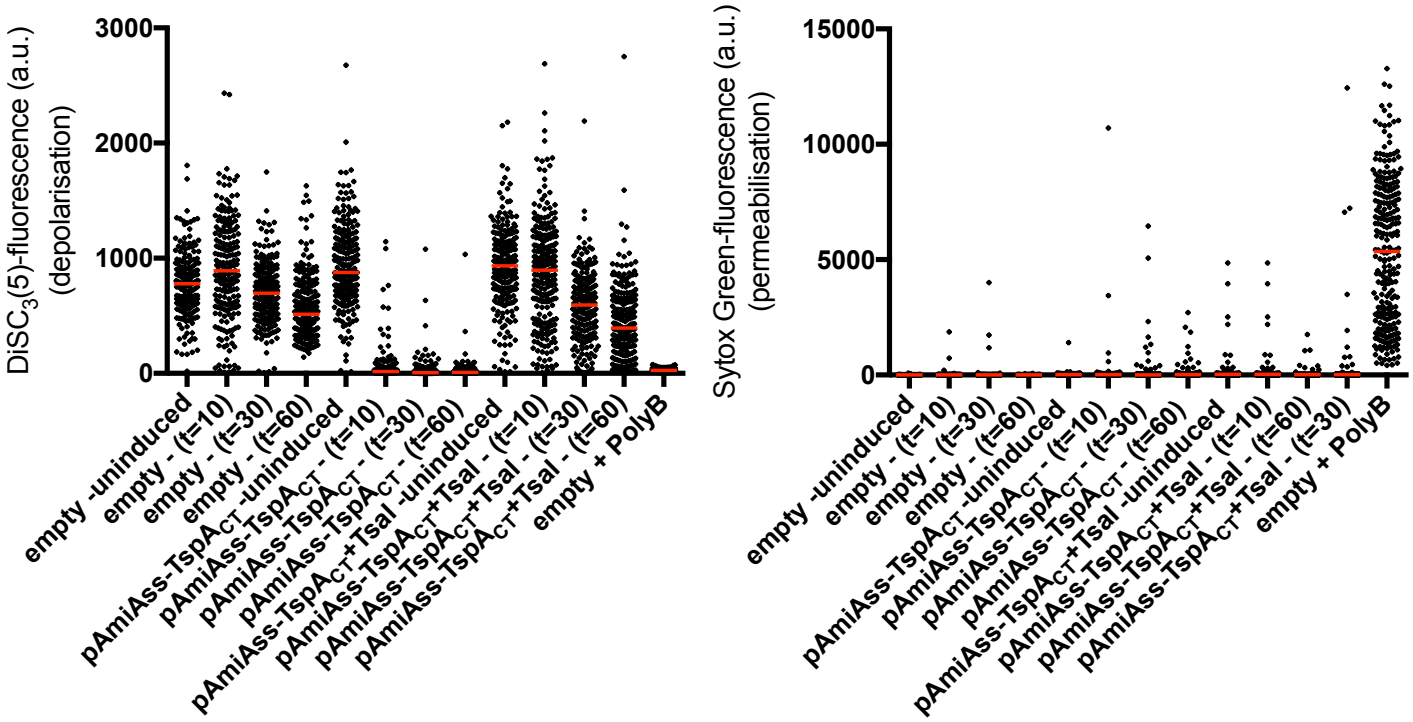

Figure S3. Rapid membrane depolarization by the C-terminal domain of TspA. Fluorescence intensity changes in $DiSC_3(5)$ (left) and Sytox Green (right) in uninduced cells harbouring pBAD18-Cm (empty), pBAD18-AmiAss-$TspA_{CT}$ and pBAD18-AmiAss-$TspA_{CT}$ and upon induction with 0.2% L-arabinose. Cells were then induced for 10, 30 and 60 minutes before samples removed and cells incubated with $DiSC_3(5)$ and Sytox Green. Fluorescence intensity of $DiSC_3(5)$ and Sytox Green also measured upon addition of Polymixin B to empty vector as a control for membrane depolarization and permeabilisation.

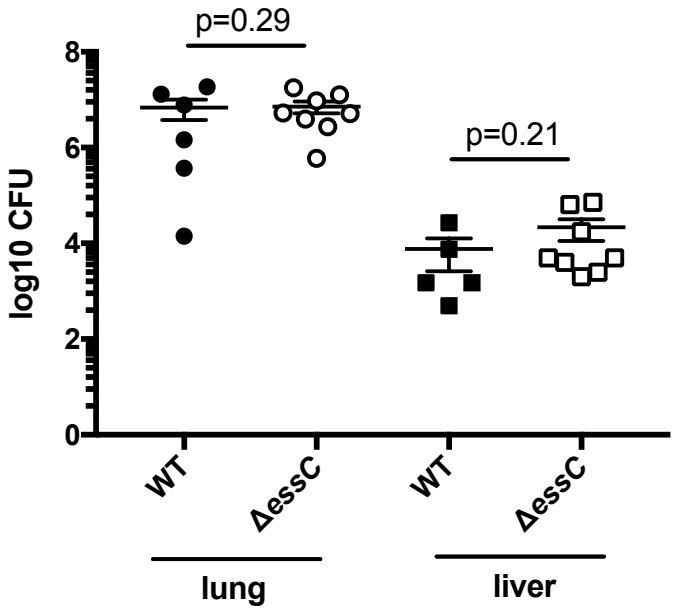

Figure S4. No difference in bacterial burden between wild type and *essC* mutant strains in a 24 hour murine pneumonia infection model. Female 10-12 week old C57/B6 mice were challenged with 3 x 10^8 cfu/ml of RN6390 (WT) or the isogenic Δ*essC* strain. Bacterial load was determined in liver and lungs 24 hours after infection. Mean ± SEM (horizontal bars) is shown. Significance testing performed by unpaired *t* test.

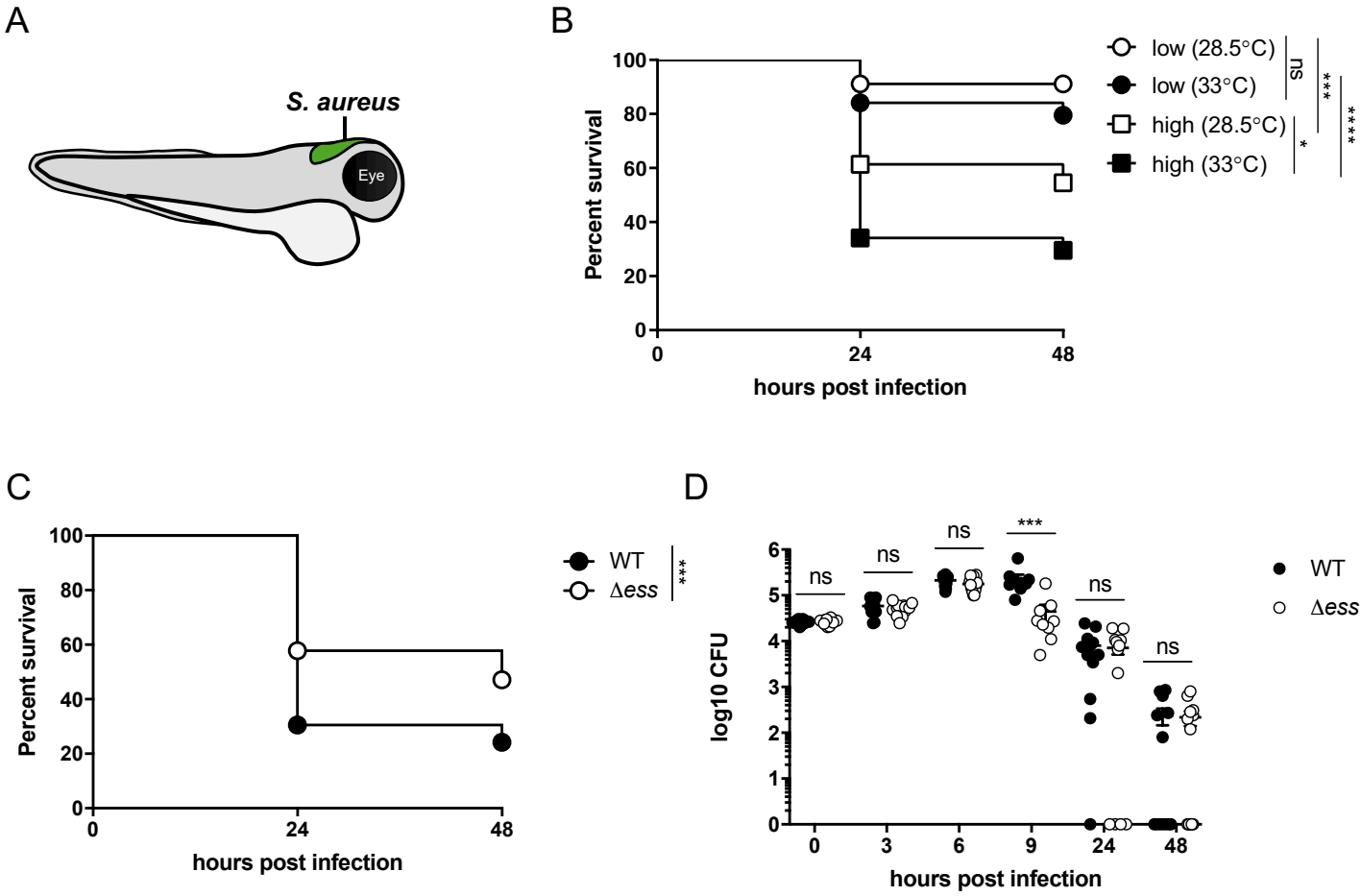

Figure S5. Developing a zebrafish model to assess T7SS activity *in vivo*. A. Schematic of zebrafish larvae showing the site of *S. aureus* injection into the hindbrain ventricle. B. Survival curves of *lyz*:dsRed zebrafish larvae injected with wild type RN6390 chromosomally tagged with GFP. Zebrafish were injected at 3 dpf with a low (~7 x 10^3 cfu), medium (~1.4 x 10^4 cfu) or high (~2 x 10^4 cfu) dose of RN6390-gfp, incubated at 28.5°C or 33°C and monitored for 48 hpi. Data are pooled from two independent experiments (*n*=22-25 larvae per experiment). Results are plotted as a Kaplan- Meier survival curve and the p value between conditions was determined by log-rank Mantel-Cox test. C. Survival curves of *lyz*:dsRed larvae infected in the hindbrain 3 dpf with RN6390-gfp or RN6390 Δ*ess*-gfp at a dose of ~2 x 10^4 cfu and incubated at 33°C for 48 hpi. Data are pooled from three independent experiments (*n*=28-50 larvae per experiment. Results are plotted as a Kaplan-Meier survival curve and the p value between conditions was determined by log-rank Mantel-Cox test. D. Enumeration of recovered bacteria at 0, 3, 6, 9, 24 or 48 hpi from zebrafish larvae infected with RN6390-gfp or RN6390 Δ*ess*-gfp. Pooled data from 3 independent experiments. Circles represent individual larva, and only larvae having survived the infection were included. Mean ± SEM also shown (horizontal bars). Significance was tested using an unpaired *t* test. **p*<0.05 ***p*<0.01, *** *p*<0.001, **** *p*<0.0001, ns, not significant.

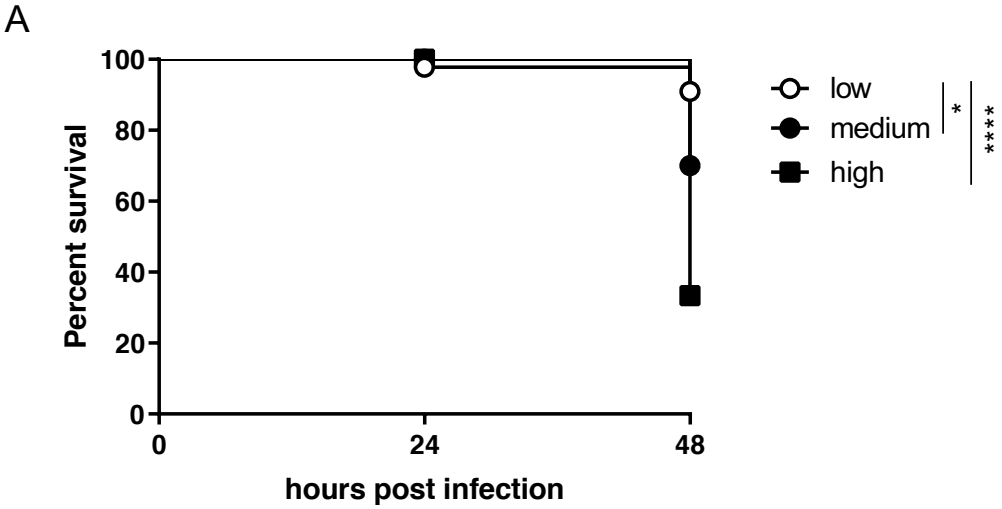

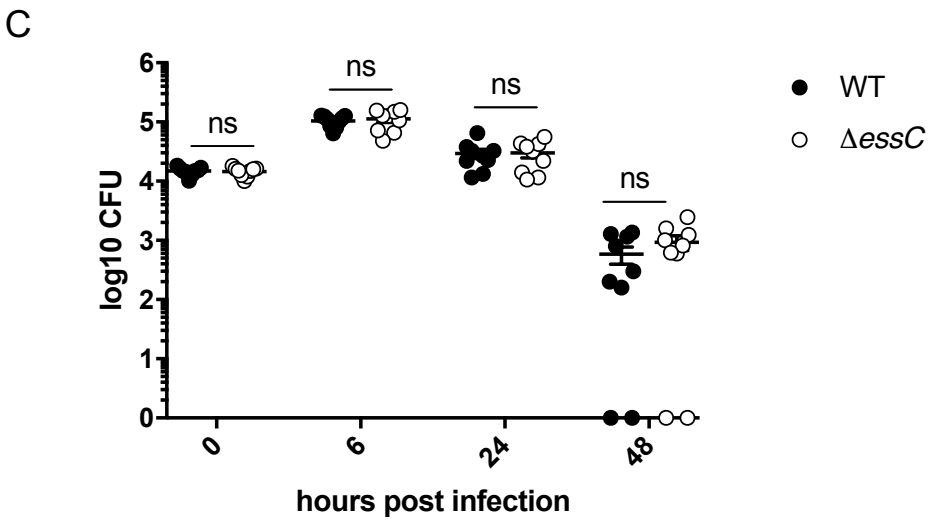

Figure S6. *S. aureus* COL also exhibits dose and T7SS-dependent zebrafish mortality. A. Survival curves of WT zebrafish larvae injected with wild type COL chromosomally tagged with mCherry. Zebrafish were injected at 3 dpf with a low (~7 x 10^3 cfu), medium (~1.5 x 10^4 cfu) or high dose (~2 x 10^4 cfu) of COL-mCherry, incubated at 33°C and monitored for 48 hpi. Data are pooled from three independent experiments. Results are plotted as a Kaplan-Meier survival curve and the *p* value between conditions was determined by log-rank Mantel-Cox test. B. Survival curves of zebrafish larvae injected in the hindbrain 3 dpf with COL-mCherry (WT) or COL Δ*essC*-mCherry at a dose of ~1.6 x 10^4 cfu and incubated at 33°C for 48 hpi. Data are pooled from three independent experiments (*n*=23-30 larvae per experiment). Results are plotted as Kaplan-Meier survival curves and the *p* value between conditions was determined by the log-rank Mantel Cox test. C. Enumeration of recovered bacteria at 0, 6, 24 or 48 hpi from zebrafish larvae infected with COL-mCherry (WT) or COL Δ*essC*-mCherry. Circles represent individual larvae and data pooled data from 3 independent experiments. Mean ± SEM also shown (horizontal bars). Significance was tested using an unpaired *t* test. **p*<0.05 ***p*<0.01, *** *p*<0.001, **** p<0.0001, ns, not significant.

A

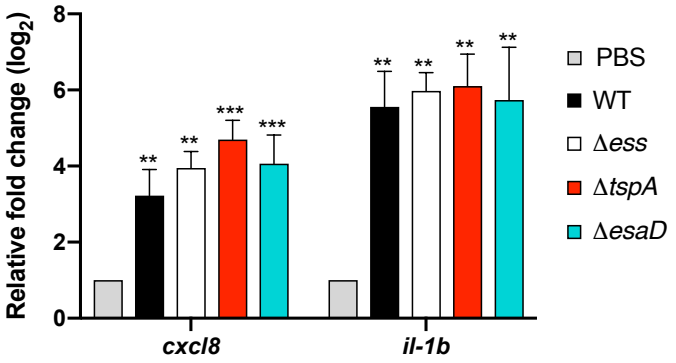

Figure S7. *S. aureus* infection elicits a strong inflammatory response independent of the T7SS. A. *S. aureus* RN6390-gfp, RN6390 Δ*ess*-gfp, Δ*tspA*-gfp or RN6390 Δ*esaD*-gfp were injected in 3 dpf zebrafish larvae at a dose of ~2 x 10^4 CFU and incubated at 33°C. Expression of *cxcl8* and *il-1b* was determined at 6 hpi when the bacterial burden between among strains was similar. Mean relative *cxcl8* and *il-1b* gene expression levels (qRT-PCR) were quantified and values were normalised to the PBS-injected larvae. Therefore, the *p* value (indicated above the bars) represents the statistical significance of the indicated *S. aureus* strains in comparison to the PBS-injected larvae. Pooled data from 4 independent experiments where 10 larvae were sacrificed after 6 hpi. Error bars represent mean with SEM (horizontal bars). Significance was performed using a one-way ANOVA with Sidak's correction. *$p<0.05$ **$p<0.01$, *** $p<0.001$, **** $p<0.0001$, ns, not significant.

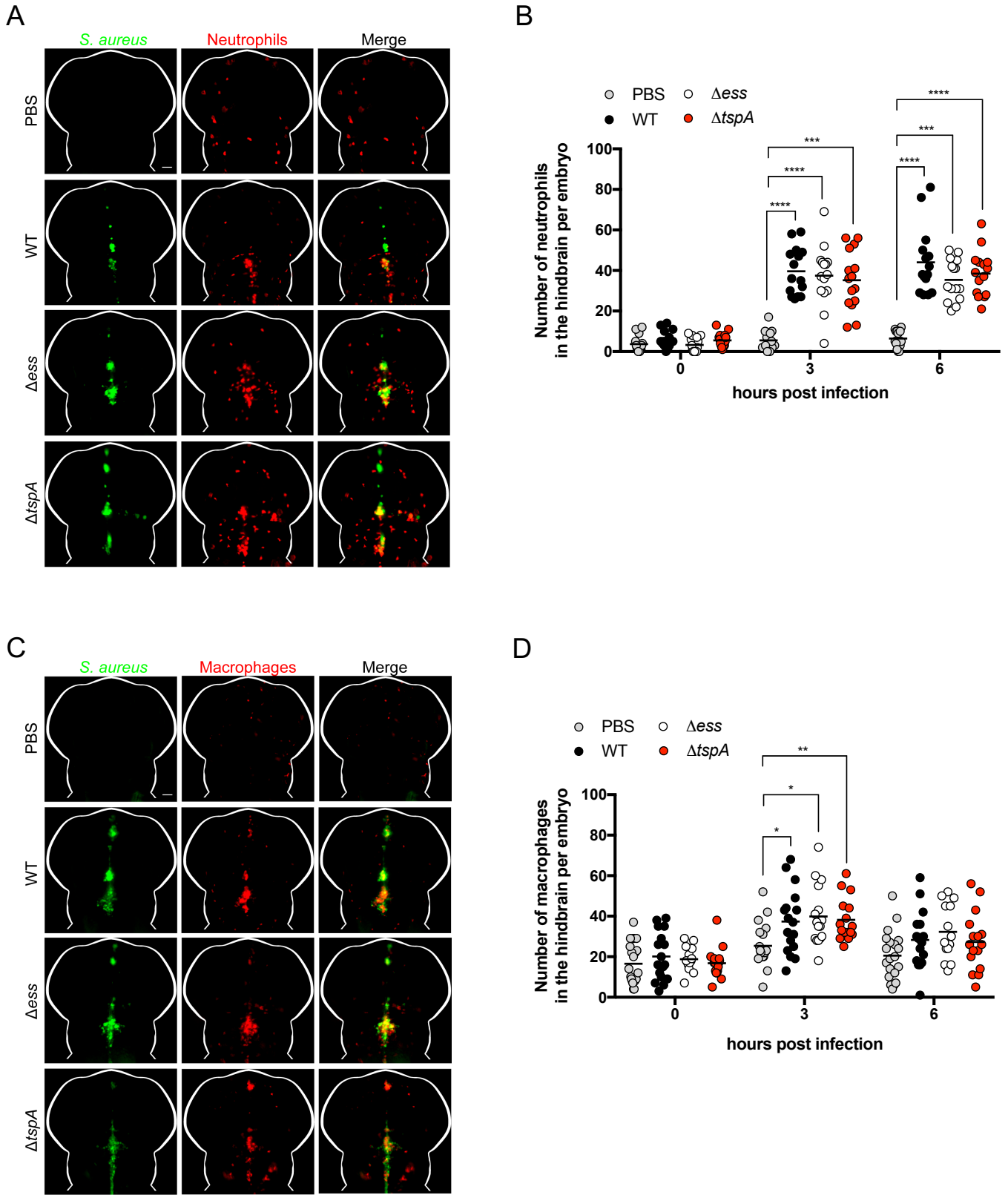

Figure S8. T7SS independent leukocyte recruitment to *S. aureus* infection. A+B. Neutrophils were imaged and counted in the whole hindbrain for Tg(*lyz*::dsRed) larvae and C+D. Macrophages were imaged and counted in the whole hindbrain for Tg(*mpeg1*::G/U::mCherry) larvae injected with PBS, RN6390-gfp, RN6390 Δ*ess*-gfp or RN6390 Δ*tspA*-gfp. Larvae were imaged using a fluorescent stereomicroscope at 0, 3 and 6 hpi and data obtained from three independent experiments with 5-6 larvae imaged per strain. Data points represent an individual larvae with the geometric mean. Significance testing performed using Kruskal-Wallis test with Dunn's correction. *$p<0.05$ **$p<0.01$, *** $p<0.001$, **** $p<0.0001$, ns, not significant. Representative images of a single z stack of neutrophil or macrophage recruitment at 6 hpi is shown in A+C, respectively. Leukocytes are labelled in red and S. aureus in green, with overlay in yellow. Scale bar = 50 µm Scale bar Scale bar = 50 µm.

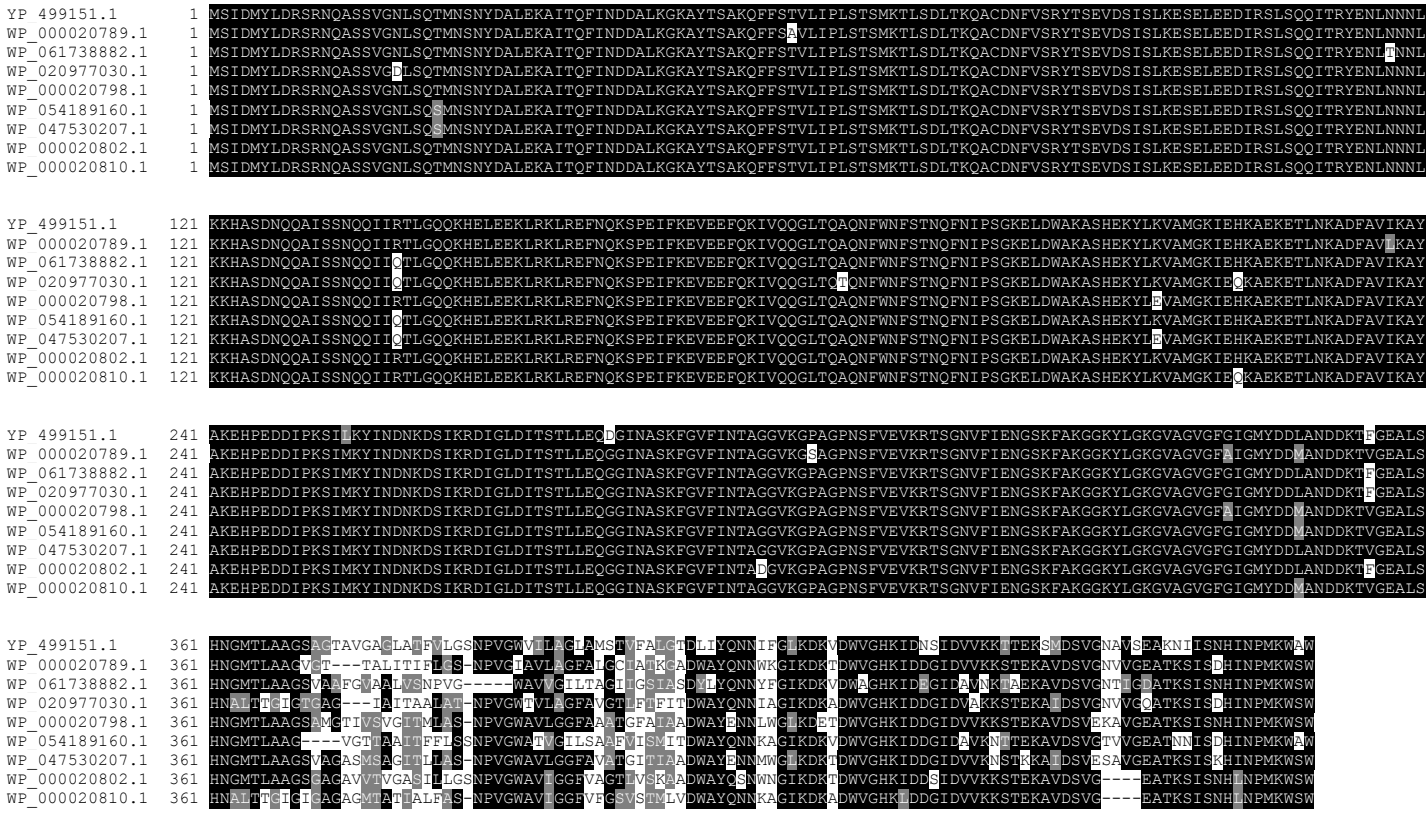

Figure S9. TspA proteins encoded by *S. aureus* strains show variability within the channel-forming domain. A selection of TspA protein sequences encoded by *S. aureus* strains were extracted from NCBI (ncbi.nlm.nih.gov/), aligned using ClustalW (http://www.ch.embnet.org/software/ClustalW.html) and shaded with Boxshade (http://www.ch.embnet.org/software/BOX_form.html).